1986

A Spectral Iterative Approach for Analyzing the Scattering of Cylindrical Waves from One Dimensional Wire Gratings

James R. Dire
University of Central Florida

A SPECTRAL ITERATIVE APPROACH FOR ANALYZING THE SCATTERING OF CYLINDRICAL WAVES FROM ONE DIMENSIONAL WIRE GRATINGS

BY
JAMES R. DIRE
B.S., Chemistry, University of Missouri, 1982
B.S., Physics and Mathematics, University of Missouri, 1982

Thesis

Submitted in partial fulfillment of the requirements
for the Master of Science degree in Physics
in the Graduate Studies Program of the
College of Arts and Sciences
University of Central Florida
Orlando, Florida

Fall Term
1986

ABSTRACT

The scattering of cylindrical waves, infinite in the axial direction, from a one dimensional infinite, planar, periodic array of wires is investigated. The cylindrical wavefront is divided into planar segments. Each planar segment is treated individually as an infinite plane wave incident upon the periodic structure. The reflection characteristics of each plane wave is determined by analyzing the electromagnetic scattered fields using the secant method to solve an iterative algorithm. The derivation of the method as applied to surfaces containing a one dimensional parallel thin wire grating is presented. The reflection coefficients for cylindrical waves are determined by combining the reflection coefficients of the planar segments. The reflection characteristics of the grating as a function of wire spacing, wire thickness and polarization of the incident field are calculated.

TABLE OF CONTENTS

LIST OF FIGURES

LIST OF TABLES

I. INTRODUCTION

In this present day and age one can hardly travel anywhere without seeing numerous types of antennas. The days of seeing simple rooftop television antennas have given away to a vast matrix of communication dishes scattered all over the countryside. As communication needs and technology continue to evolve so does the research in antenna theory.

Many types of antenna dishes are currently available, each having its own particular advantages and disadvantages. Solid parabolic dishes tend to require larger structural support but tend to be more efficient in that less signal power is lost with the reflection off the dish. On the other hand wire mesh antenna dishes are considerably less massive. They are less expensive per area of aperture and do not require as extensive structural support. They do, however, suffer from greater signal power losses than solid reflecting surfaces due to their lower reflection coefficients.

For space applications, wire mesh antennas are desirable for many reasons. First, although all antennas in space are weightless, wire mesh antennas with their smaller mass per aperture are deployed at a much lower cost.

Secondly, these type of antennas can sometimes be folded for compactness during transportation. Again, however, in space applications one must consider that signal power reflection is lower for wire array antennas than for solid reflectors. Because of this, much research has been done in analyzing the reflection of electromagnetic waves from wire mesh antennas.

The problem of analyzing the interaction of electromagnetic waves with wire mesh antennas is simply a scattering problem of electromagnetic waves from a periodic array of conductors. One of the first works done on the theory of scattering from a parallel wire grating was done by Wait [1]. An excellent review of most of the work done prior to 1960 in wire grating theory was published by Larsen [2].

Many different methods have been developed for solving the problem of electromagnetic scattering from such structures. The best known method, called the Method of Moments, tend to require the inversion of large matrices and thereby uses a large quantity of computer time and memory. Current approaches to solving the scattering from wire gratings utilize iterative techniques to determine the scattered fields and induced wire currents. An approach that alleviates the usage of large quantities of memory, developed by Tsao and Mittra [3], is called the Spectral Iteration Approach (SIT). Their approach worked well when

the wavelength of the radiation was less than half the separation of the wires in the grating (e.g., infrared and microwave regions of the electromagnetic spectrum). However, their approach failed to converge when the wavelength was greater than half the periodic spacings (e.g. radio wavelengths).

Brand [4] applied a contractor corrector scheme to the Spectral Iteration Approach. This eliminated the convergence failures of the previous SIT method. Christodoulou [5], like Brand, developed another method which eliminated the convergence problems encountered by Tsao and Mittra. His method, called the Fast Fourier Transform Conjugate Gradient Method (FFT-CG), is a combination of the SIT and the Conjugate Gradient Method [6,7].

All of the above SIT methods were developed to achieve more efficient numerical calculations of the solutions of wire grating scattering problems. They all make use of convergence techniques that involve calculating derivatives and all incorporate a Fast Fourier Transform (FFT) to quickly solve the iterative scheme developed by Tsao and Mittra.

Virtually all previous investigations in the scattering of electromagnetic waves from wire gratings have involved the study of plane waves incident upon planar structures. The simplicity of this geometry makes the development of numerical techniques much easier. Such solutions have

practical uses in that when transmitter and detector distances from wire gratings are much larger than the wavelengths and wire spacings, the wavefronts are essentially planer when arriving at the array. The purpose of this research, however, is to analyze the scattering of cylindrical waves. There exist many types of antennas in which the wavefronts are cylindrical or spherical and far field planar approximations do not hold. The intent is that if a workable technique for the solution of the scattering problem is developed for cylindrical waves, infinite in the axial direction and incident on a one dimensional infinite planar periodic wire grating, then even more complicated geometries can be investigated.

II. FORMULATION OF THE SPECTRAL ITERATION

To derive the iterative equation to solve for the electromagnetic fields and current densities, consider the generalized integral expression for a scattering problem:

$$\Phi(\vec{r}) = \int G(\vec{r},\vec{r}')\Psi(\vec{r}')d\vec{r}' + \Phi_{inc}(\vec{r}) \qquad (2.1)$$

subject to the constitutive equation:

$$\Psi(\vec{r}) = K(\vec{r}) \Phi(\vec{r}) \qquad (2.2)$$

Here $\Phi(\vec{r})$ is the field quantity, $\Psi(\vec{r})$ the source density and $\Phi_{inc}(\vec{r})$ the externally applied field. $G(\vec{r},\vec{r}')$ is the appropriate Green's function.

This equation can be solved by application of transform techniques. The Fourier transform of a function is given by:

$$\tilde{F}(\vec{k}) = \int_{-\infty}^{\infty} f(\vec{r})\, e^{j\vec{r}\cdot\vec{k}}\, d\vec{r} \qquad (2.3)$$

All transform pairs will be denoted in the form $\tilde{F}(\vec{k}) \leftrightarrow f(\vec{r})$.

Taking the Fourier transform of equation (2.1) gives:

$$\mathcal{F}(\vec{k}) = \mathcal{G}(\vec{k}) \quad \mathcal{F}(\vec{k}) \quad + \quad \mathcal{F}_{inc}(\vec{k}) \tag{2.4}$$

which is still subjected to the conditions of the constitutive equation. The integral equation has been converted into an algebraic equation in the transform space where a solution can be more readily obtained. This procedure is now applied to the problem of scattering of electromagnetic waves from a periodic structure (see Figure 1).

The electric field $\vec{E}$ arising from a magnetic current $\vec{M}$ is given by:

$$\vec{E} = - (1/\varepsilon) \nabla \times \vec{F} \tag{2.5}$$

where $\vec{F}$ is the associated electric vector potential and ε the permittivity of the medium. The relationship between $\vec{F}$ and $\vec{M}$ is:

$$\vec{F} (\vec{r}) = \varepsilon \int \bar{\bar{G}} (\vec{r},\vec{r}') \vec{M}(\vec{r}') \, d\vec{r}' \tag{2.6}$$

where $\bar{\bar{G}}(\vec{r},\vec{r}')$ is the free space Green's function defined by:

$$\bar{\bar{G}}(\vec{r},\vec{r}') = e^{-j(\hat{r}\cdot\hat{k})} \quad \bar{\bar{I}} / 4 \pi r \tag{2.7}$$

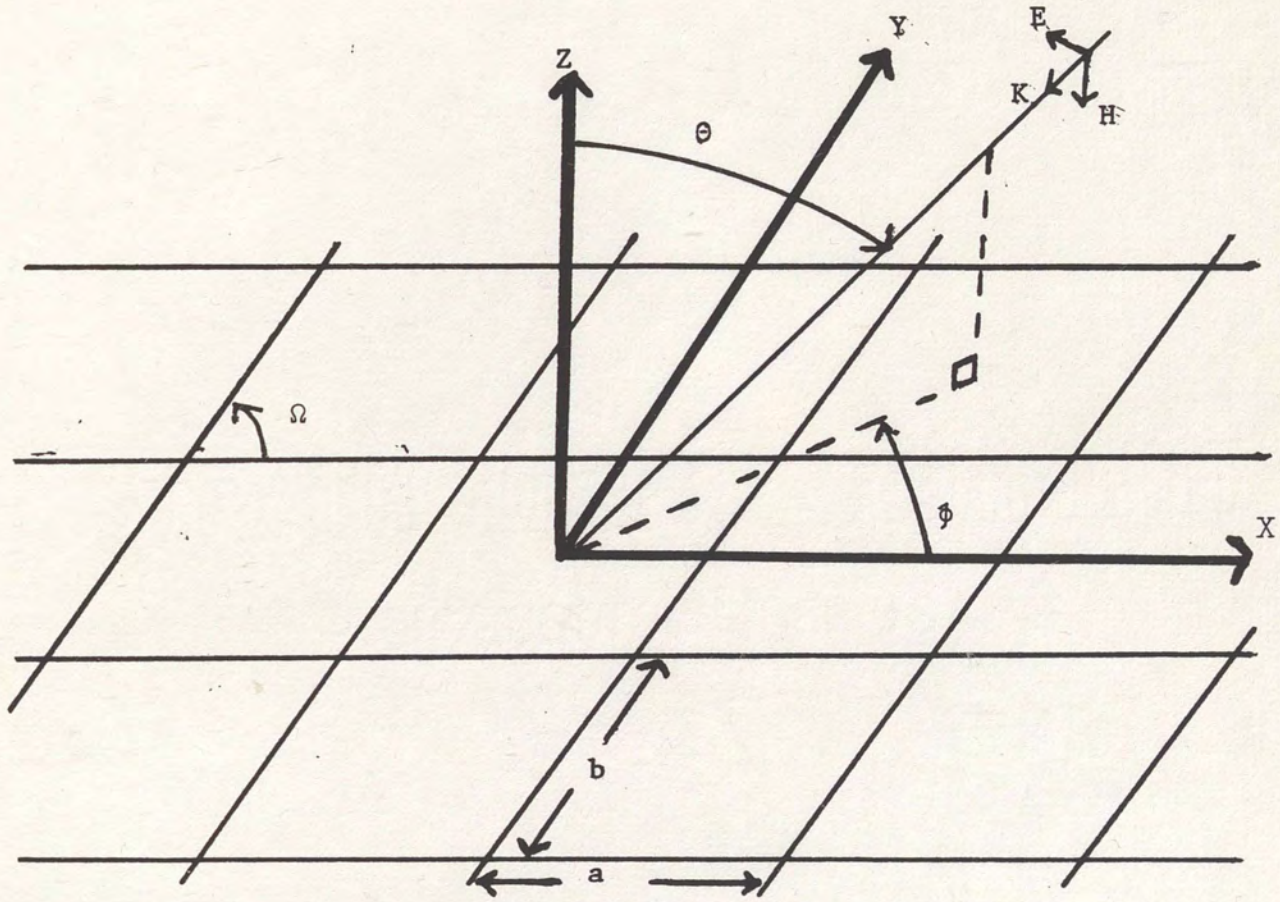

Figure 1. Geometry of the Scattering Problem.

$\bar{\bar{I}}$ being the unit dyadic.

Since all the fields and sources are harmonic with frequency ω, equation (2.5) can be substituted into one of Maxwell's equations:

$$\nabla \times \vec{H} = \partial \vec{E}/\partial t = j\,\omega\,\varepsilon\,\vec{E} \tag{2.8}$$

to yield:

$$\nabla \times \vec{H} = -\,j\,\omega\,\nabla \times \vec{F} \tag{2.9}$$

or:

$$\nabla \times (\vec{H} + j\,\omega\,\vec{F}) = 0 \tag{2.10}$$

This implies $\vec{H} + j\,\omega\,\vec{F}$ is a gradient of some scalar potential.

$$-\nabla \Phi_m = \vec{H} + j\omega\,\vec{F} \quad \text{or} \quad \vec{H} = -\,j\,\omega\,\vec{F} - \nabla \Phi_m \tag{2.11}$$

where Φ_m is the magnetic scalar potential.

To specify a vector completely, both its divergence and curl must be defined. Equation (2.5) defines the curl of vector $\vec{F}$. To define its divergence the Lorentz guage condition is used:

$$\nabla \cdot \vec{F} + \varepsilon \mu \, \partial \Phi_m / \partial t = 0 \qquad (2.12)$$

where μ is the permeability of the medium. Since Φ_m is harmonic (i.e., $\exp(-j\omega t)$ dependence) equation (2.12) becomes:

$$\nabla \cdot \vec{F} = - j \omega \varepsilon \mu \, \Phi_m \qquad (2.13)$$

which gives:

$$\Phi_m = \frac{-1}{j\omega\varepsilon\mu} \nabla \cdot \vec{F} \qquad (2.14)$$

Equation (2.14) can be substituted into equation (2.11) to yield:

$$\vec{H} = - j \omega \vec{F} + \frac{1}{j\omega\varepsilon\mu} \nabla \nabla \cdot \vec{F} \qquad (2.15)$$

Equation (2.15) can now be applied to the planar periodic structure of Figure 1, where the structure is considered to be the source distribution for the magnetic field. Since the wire array resides entirely in the x-y plane the vector potential is not a function of the z coordinate. If the medium is free space ε becomes ε_o and μ becomes μ_o. With the propagation constant defined by $k_o = \omega(\mu_o \varepsilon_o)^{1/2}$ equation (2.15) becomes:

$$\vec{H}_s(x,y) = {}^{1}/_{j\omega\mu_o\varepsilon_o}\{ (k_o^2 F_x + {}^{\partial^2 F_y}/_{\partial x\partial y} + {}^{\partial^2 F_x}/_{\partial x^2})\,\hat{x}$$

$$+ (k_o^2 F_y + {}^{\partial^2 F_x}/_{\partial x\partial y} + {}^{\partial^2 F_y}/_{\partial y^2})\,\hat{y}\ \} \qquad (2.16)$$

The subscript "s" is to be interpeted as the scattered field.

In vector notation equation (2.16) is expressed as:

$$\vec{H}_s(x,y) = \begin{bmatrix} H_x \\ H_y \end{bmatrix} = \frac{1}{j\omega\varepsilon_o\mu_o} \begin{bmatrix} k_0^2 + {}^{\partial^2}/_{\partial x^2} & {}^{\partial^2}/_{\partial x\partial y} \\ {}^{\partial^2}/_{\partial x\partial y} & k_o^2 + {}^{\partial^2}/_{\partial y^2} \end{bmatrix} \begin{bmatrix} F_x \\ F_y \end{bmatrix} \qquad (2.17)$$

When equation (2.6) is substituted into equation (2.17) and the Fourier transform is taken, the scattered field becomes in the transform space:

$$\tilde{\tilde{H}}_s(\alpha_{mn},\beta_{mn}) = \{1/_{j\omega\,\mu_o}\} \quad X$$

$$\begin{bmatrix} k_0^2 - \alpha_{mn}^2 & \alpha_{mn}\beta_{mn} \\ -\alpha_{mn}\beta_{mn} & k_o^2 - \beta_{mn}^2 \end{bmatrix} \quad \tilde{\tilde{G}}(\alpha_{mn},\beta_{mn}) \quad \tilde{\tilde{M}}(\alpha_{mn},\beta_{mn}) \qquad (2.18)$$

The discrete nature of equation (2.18) is the result of taking the Fourier Transform of a periodic function. The parameters α_{mn} and β_{mn} are called the Floquet modes. The Floquet modes allow for the coupling between the conducting regions of the planar array [8,9,10].

They are defined as:

$$\alpha_{mn} = \frac{2\pi m}{a} - k_o \sin\theta \cos\phi \tag{2.19}$$

$$\beta_{mn} = \frac{2\pi n}{b} - \frac{2\pi m}{a} \cot\Omega - k_o \sin\theta \sin\phi \tag{2.20}$$

The parameters a and b, and the angles θ, ϕ, and Ω are shown in Figure 1. The parameters m and n are the number of sampling points in the x and y directions, respectively, used in the Fast Fourier Transform.

The Fourier transform of the Green's function is given by:

$$\tilde{\bar{G}} = \frac{-j}{2} \left(k_o^2 - \alpha_{mn}^2 - \beta_{mn}^2 \right)^{-1/2} \bar{\bar{I}} \tag{2.21}$$

Equation (2.18) gives the scattered aperture field in the transform space. Taking the inverse Fourier transform yields:

$$\bar{\bar{H}}_s(x,y) = \left(\frac{1}{j\omega\mu_o} \right) \sum_{m,n} \begin{vmatrix} k_o^2 - \alpha_{mn}^2 & \alpha_{mn}\beta_{mn} \\ -\alpha_{mn}\beta_{mn} & k_o^2 - \beta_{mn}^2 \end{vmatrix} \tag{2.22}$$

$$\times \quad \bar{\bar{G}}(\alpha_{mn},\beta_{mn}) \; \bar{\bar{M}}(\alpha_{mn},\beta_{mn}) \exp\{j(\alpha_{mn}x + \beta_{mn}y)\}$$

This is the scattered aperture field in terms of the magnetic current density. By the use of the equivalence theorem and applying the appropriate bounary condition on $\vec{H}_s(x,y)$ at z=0 equation (2.22) becomes [3]:

$$\vec{H}_t^{inc} = \frac{-2}{j\omega\mu_o} \sum_{m,n} \begin{bmatrix} \alpha_{mn}\beta_{mn} & k_o^2-\alpha_{mn}^2 \\ -k_0^2+\alpha_{mn} & -\alpha_{mn}\beta_{mn} \end{bmatrix} \quad (2.23)$$

$$X \quad \bar{\bar{G}}(\alpha_{mn},\beta_{mn})\ \tilde{\bar{E}}(\alpha_{mn},\beta_{mn})\ \exp\{j(\alpha_{mn}x+\beta_{mn}y)\}$$

where $\tilde{\bar{E}}$ represents the transformed aperture electric field and $\vec{H}_t^{inc}$ is the incident tangential magnetic field.

It should be noted that equation (2.23) only applies in the aperture region. To extend the equation to apply over the full range, that is , encompassing an entire unit cell, the contribution of the $\vec{H}$ field along the conducting wires has to be added to the equation. This gives:

$$\Theta_c\{\vec{J}(x,y)\} = \vec{H}_t^{inc} + \frac{2}{j\omega\mu_o} \sum_{m,n} \begin{bmatrix} \alpha_{mn}\beta_{mn} & k_o^2-\alpha_{mn}^2 \\ -k_o^2+\beta_{mn}^2 & -\alpha_{mn}\beta_{mn} \end{bmatrix}$$

$$X \quad \bar{\bar{G}}(\alpha_{mn},\beta_{mn})\ \tilde{\bar{E}}(\alpha_{mn},\beta_{mn})\ \exp\{j(\alpha_{mn}x+\beta_{mn}y)\} \quad (2.24)$$

The truncation and complimentary trunction operators, Θ and Θ_c , are defined by:

$$\Theta\{f(\vec{r})\} = f(\vec{r}) \quad \text{for} \quad \vec{r} \quad \text{in the aperture}$$

$$= 0 \quad \text{for} \quad \vec{r} \quad \text{in the conduction region}$$

$$\Theta_c\{f(r)\} = 0 \quad \text{for} \quad \vec{r} \quad \text{in the aperture}$$

$$= f(\vec{r}) \quad \text{for} \quad \vec{r} \quad \text{in the conducting region}$$

$\Theta_c\{J(x,y)\}$ is present on equation (2.24) since the current densities can only be present in the conducting regions. The identity that $\hat{Z} \times \{\vec{H}(z=o^+) - \vec{H}(z=0^-)\} = \vec{J}$ is used in equation (2.24).

Equation (2.24) can be written in a more compact form if the following definition is made:

$$\overline{\overline{G}}_o = \begin{bmatrix} \alpha_{mn}\beta_{mn} & k_o^2 - \alpha_{mn}^2 \\ -k_o^2 + \beta_{mn}^2 & \alpha_{mn}\beta_{mn} \end{bmatrix} \quad \overline{\overline{G}}(\alpha_{mn}, \beta_{mn}) \tag{2.25}$$

This gives:

$$\Theta_c(\vec{J}) = \vec{H}_t^{inc} + \frac{2}{j\omega\mu_o} \sum_{m,n} \overline{\overline{G}}_o \; \overline{\overline{E}}_t \; \exp\{j(\alpha_{mn}x + \beta_{mn}y)\} \tag{2.26}$$

Recall the subscript t indicates the tangential component and it is understood all quantities are evaluated at z=0.

Equations (2.18) through (2.26) assume the geometry of Figure 1. The equations simplify considerably if instead of a two dimensional wire grid a one dimensional wire grating

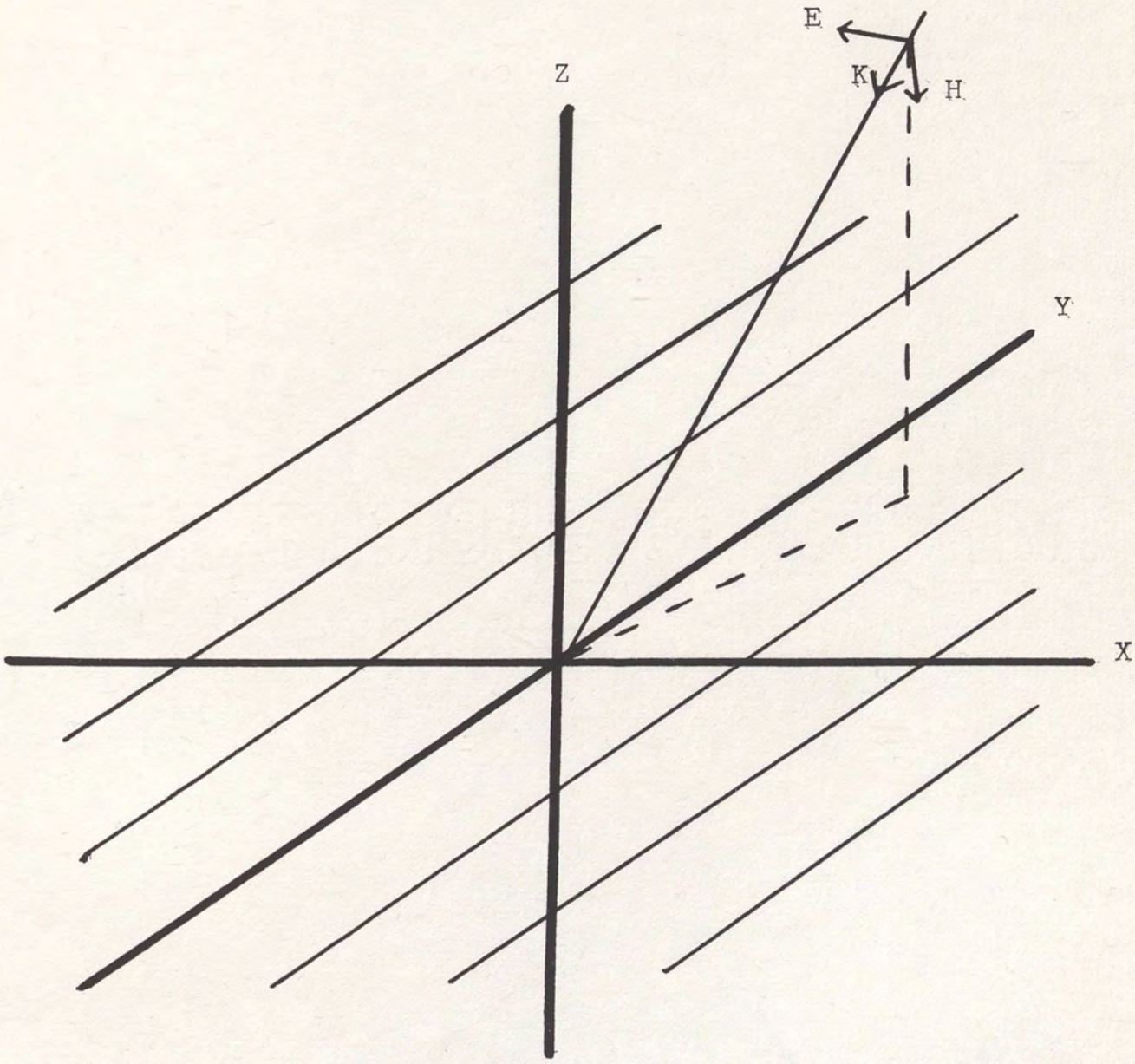

Figure 2. One Dimensional Wire Array.

is used (Figure 2). If $\Omega = 90^{o}$, $b = -\infty$, and one only considers transverse electric polarization (i.e., $\phi = 0$), then $\beta_{mn} = 0$ and equations (2.18), (2.22), (2.23), and (2.24) no longer contains the 2x2 matrix. Equation (2.26) still holds as a general equation and is the equation to be solved by iterative techniques.

The derivation of the iterative method used by Tsao and Mittra proceeds as follows: Since the tangential field is only present in the aperture and the current densities only along the conductor, equation (2.26) can be written as:

$$\Theta_c(\vec{J}) = \Theta_c \{ \vec{H}_t^{inc} + (2/j\omega\mu_o) F^{-1}(\tilde{\tilde{G}}_o F\{\Theta(\vec{E}_t)\})\} \qquad (2.27)$$

Similarly equation (2.26) can be solved for $\vec{E}_t$ and expressed as:

$$\vec{E}_t = F^{-1}\{ \tilde{\tilde{G}}_o^{-1} F \ (j\omega\mu_o/2) \ (\Theta_c(\vec{J}) - \vec{H}_t^{inc}) \} \qquad (2.28)$$

Equation (2.27) expresses the current densities in terms of the cell electric field, whereas equation (2.28) gives the electric field in terms of the incident tangential magnetic field and the current densities. Neither equation can be solved separately, however, substitution of equation (2.27) into equation (2.28) yields the following iterative

equation which can be solved using various numerical techniques.

$$\vec{E}_t^{(i+1)} = F^{-1}\left[\tilde{\tilde{G}}_o\, F\left\{(j\omega\mu_o/2)\left[\Theta_c\{\, H_t^{inc} + (2/j\omega\mu_o)\right.\right.\right.$$

$$\left.\left.\left. F^{-1}\left[\tilde{\tilde{G}}_o\, F\{\,(\vec{E}_t^{(i)})\}\right]\,\right\}\right] - \vec{H}_t^{inc}\,\right\}\Bigg] \tag{2.29}$$

III. CONVERGENCE OF THE ITERATIVE EQUATION

As stated in the previous chapter equation (2.29) lends itself to solution using iterative numerical techniques. This chapter explores some of the iterative techniques used to solve equation (2.29).

Most of the useful methods for solution of an equation of the form

$$F(x)=0 \tag{3.1}$$

involve iterative processes in which an initial guess i_o for a root $x=a$ is obtained by a graphical method, by the physical nature of the problem, or by some other technique. Then a recursion relationship is used to generate a sequence of successive approximations $i_1, i_2, i_3, \ldots, i_n$, which converge (under certain conditions) to a root 'a'. One such method of successive substitutions is to rewrite equation (3.1) as

$$x = F(x) \tag{3.2}$$

and make use of of a simple recursion relation

$$i_{n+1} = F(i_n) \tag{3.3}$$

There are many ways of rewriting (3.1) in the form of (3.2). The convergence, or lack thereof, of a root 'a' depends on the particular form chosen. To compare the speed of convergence of different choices of equation (3.2) the order of convergence is defined as:

$$\lim_{n \to \infty} \frac{| i_{n+1} - a |}{| i_n - a |^p} = C \qquad (3.4)$$

where C is called the asymptotic error constant and p is the order of convergence. If convergence is to take place the order of convergence must be at least 1 (linear). The magnitude of p gives an indication as to how fast convergence can take place.

One fixed point method with order of convergence equal to unity is called the method of Regula Falsi (Figure 3). Given a function f(x) on an interval $[a_i, b_i]$ such that $f(a_i)f(b_i) < 0$ then the next approximation of the solution is calculated using:

$$c = b_i - f(b_i) \frac{(b_i - a_i)}{f(b_i) - f(a_i)} = \frac{f(b_i)\, a_i - f(a_i) b_i}{f(b_i) - f(a_i)} \qquad (3.5)$$

If $f(a_i)f(c) \leq 0$ then set $a_{i+1} = a_i$ and $b_i = c$, otherwise set $a_{i+1} = c$ and $b_{i+1} = b_i$. The calculation is then repeated until a desired minimum error condition is reached. The method of Regula Falsi always keeps the root bracketed by a_i

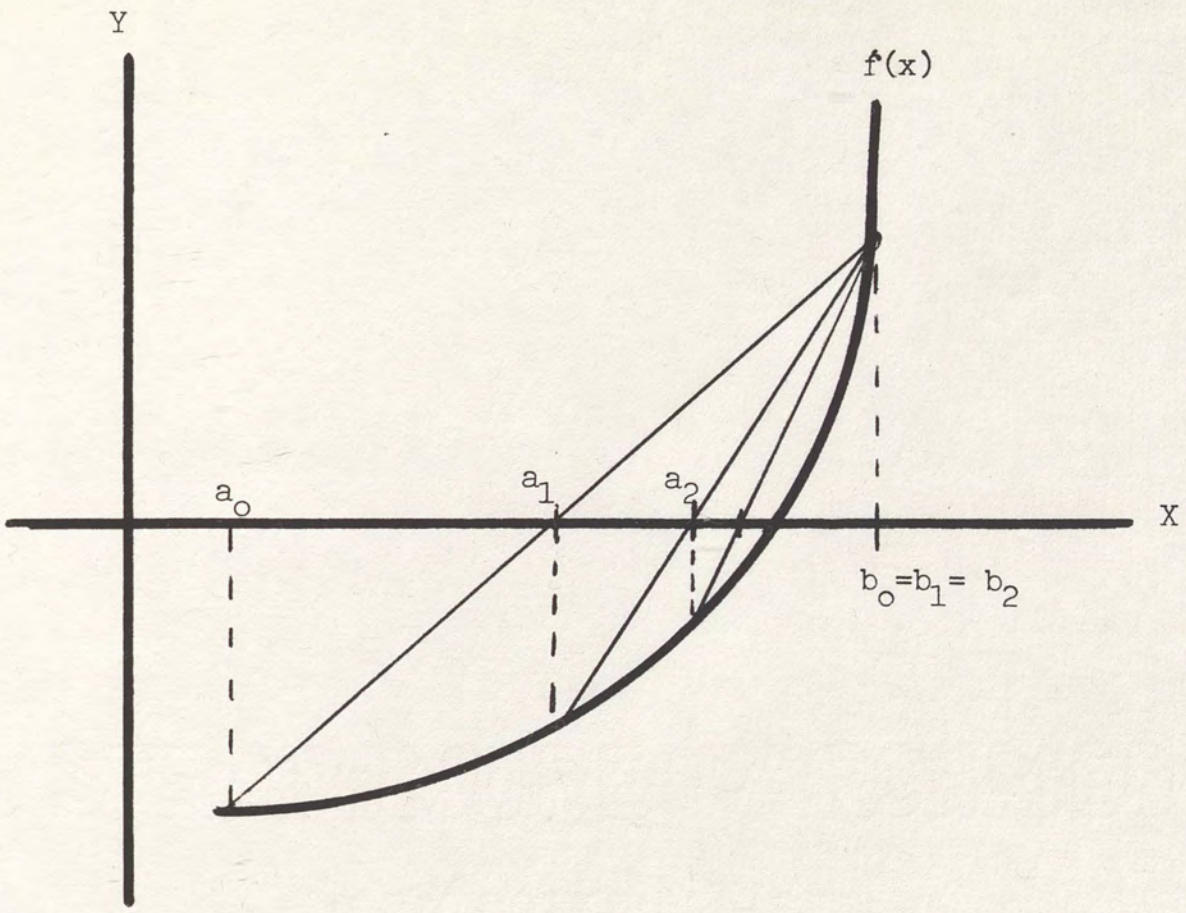

Figure 3. Method of Regula Falsi.

and b_i and the convergence is considered to be relatively slow.

Some methods of convergence make use of derivatives. The most popular of these is known as the Newton-Raphson method. The Newton-Raphson method is popular due to its simplicity and greater than unity order of convergence. This method was used by Brand to solve equation (2.29) and is discussed below.

Given a function f(x) continuously differentiable at x_i, the Newton-Raphson method (see Figure 4) calculates x_{i+1} as follows:

$$x_{i+1} = x_i - f(x_i) / f'(x_i) \qquad (3.6)$$

The Newton-Raphson method makes use of the tangent to the function at $f(x_i)$ to find the value of x_i. The solution is converged upon rapidly in a direct manner and depending on the nature of f(x), a pair of consecutive iteration may or may not bracket the root. The order of convergence of the Newton-Raphson method is 2 [11].

Another very popular convergence technique is the secant method (Figure 5). The secant method is a modification of the method of Regula Falsi which gives up bracketing of the root but has order of convergence of 1.62 [11]. In the secant method each successive approximation is calculated using the last two approximations. Given a

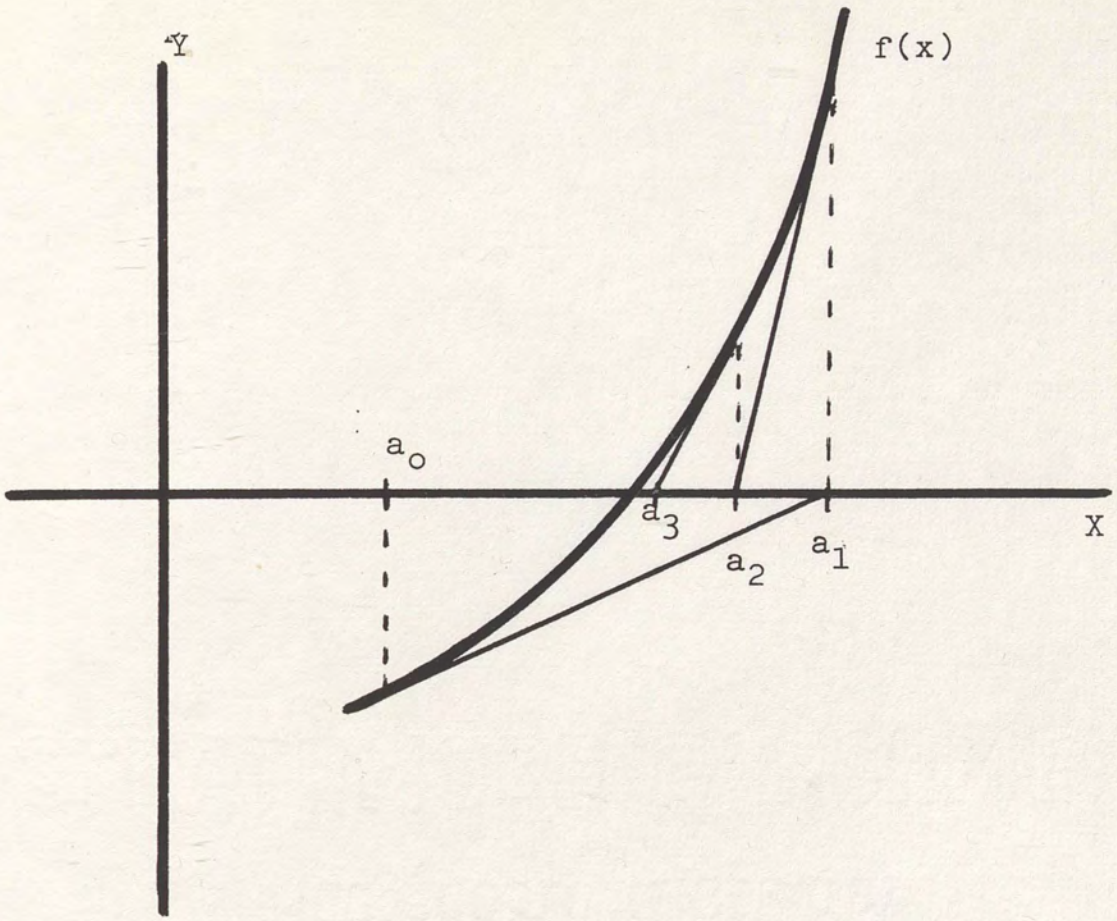

Figure 4. Newton- Raphson Method.

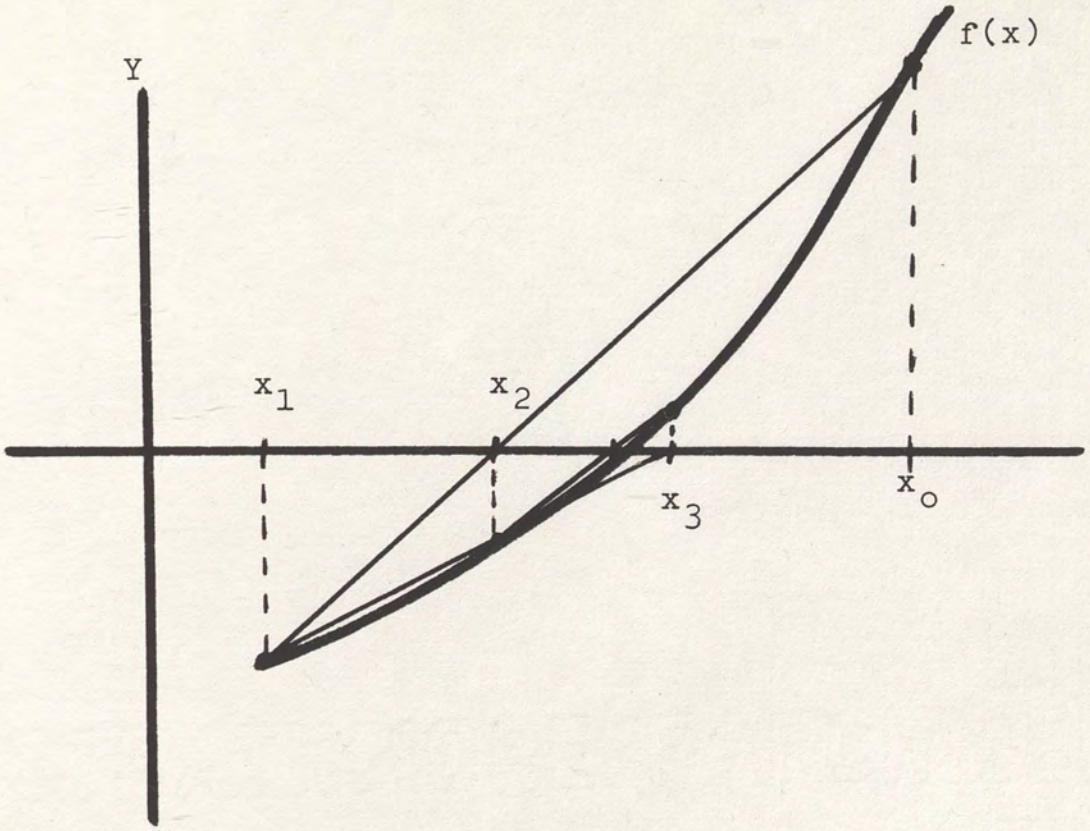

Figure 5. Secant Method.

function f(x) and two points x_i and x_{i-1} then x_{i+1} is given by:

$$x_{i+1} = \frac{f(x_i)\, x_{i-1} - f(x_{i-1})\, x_i}{f(x_i) - f(x_{i-1})} = x_i - f(x_i)\, \frac{x_i - x_{i-1}}{f(x_i) - f(x_{i-1})} \qquad (3.7)$$

Comparing the secant method to the Newton-Raphson method, the secant method only requires evaluation of one function per step while the Newton-Raphson method requires two functions be evaluated per step. The Newton-Raphson method usually converges in less iterations since the order of convergence is 2 versus 1.62 for the secant method. The secant method can often reach convergence in less computational time since no derivatives, thus less functions, need to be evaluated.

In many different problems, regardless of the convergence methods chosen, it is possible to accelerate the convergence using what are called relaxation methods. In the relaxation process, invented by Gauss, the x_i approximation is modified using a relaxation constant or residue, R. The rapidity of convergence depends on the ingenuity of the user.

With convergence techniques in mind the solution of equation (2.32) is now discussed. Recall

$$\vec{E}_t^{(i+1)} = F^{-1}\left[\tilde{\tilde{G}}_o^{-1} F\{(j\omega\mu_o/2)\left[\Theta_c\{\vec{H}_t^{inc} + (2/j\omega\mu_o) F^{-1}\left[\tilde{\tilde{G}}_o F\{\Theta(\vec{E}_t^{(i)})\}\right]\}\right] - \vec{H}_t^{inc}\}\right] \quad (2.29)$$

where

$$\Theta_c(\vec{J}) = \Theta_c\left[\vec{H}_t^{inc} + (2/j\omega\mu_o) F^{-1}\{\tilde{\tilde{G}}_o F\left[\Theta(\vec{E}_t)\right]\}\right] \quad (2.27)$$

The solution used by Tsao and Mittra involved:

1. Make an initial guess of $\vec{E}_t^{(0)}$ .Truncate $\vec{E}_t^{(0)}$.
2. Compute $\tilde{\tilde{E}}_t^{(0)}$, the Discrete Fourier Transform (DFT) of $\vec{E}_t^{(0)}$, to be carried out using the Fast Fourier Transform (FFT) algorithm.
3. Compute $\tilde{\tilde{G}}_o \cdot \tilde{\tilde{E}}^{(0)}$.
4. Obtain the inverse DFT of $\tilde{\tilde{G}}_o \cdot \tilde{\tilde{E}}^{(0)}$ using the FFT.
5. Add $\vec{H}_t^{inc}$ to the result of 4. This gives the zeroth order approximation solution $\vec{J}^{(0)}$.
6. Subtract $\vec{H}_t^{inc}$ from the complimentary truncation of the result of 5 and take the DFT using the FFT.
7. Multiply $\tilde{\tilde{G}}^{-1}$ by the last step obtaining $\tilde{\tilde{E}}^{(1)}$.
8. Take the inverse DFT of $\tilde{\tilde{E}}^{(1)}$ using the FFT to obtain $\vec{E}_t^{(1)}$.

$\vec{E}_t^{(1)}$ can then be used to find $\vec{J}^{(1)}$, then $\vec{E}^{(2)}$, etc., until the desired convergence is obtained.

The exact solution of $\vec{J}^{(i)}$ should have the entire current confined to the conducting surfaces. The exact solution of $\vec{E}_t^{(i)}$ should have zero value on the

conducting surfaces. One of the above criteria can serve as a boundary condition for checking how well the i^{th} iteration approximates the solution and an error for convergence can be established.

Tsao and Mittra had convergence problems when the separation of two wires was less than two wavelengths. Brand was able to overcome the convergence problems of Tsao and Mittra by using a relaxation technique. Given that x_{i+1} is calculated by some function $g(x_i)$ the relaxed iterative equation used was:

$$G(x_i) = R\, x_i + (1 - R)\, g(x_i) \tag{3.8}$$

R is the relaxation constant and can be optimized by the condition :

$$d/dx \; G(x)\Big|_{x=x_i} = 0 \tag{3.9}$$

This leads to:

$$R = g'(x) / \{g'(x) - 1\} \tag{3.10}$$

where $$g'(x) = d/dx \; g(x)\Big|_{x=x_i} . \tag{3.11}$$

In terms of the electromagnetic equations a new approximation of the solution $\vec{E}_t^{(i+1)}$ can be found from $\vec{E}^{(i)}$ using:

$$\vec{E}_t^{(i+1)} = \vec{R}^{(i)} \cdot \vec{E}^{(i)} + (\bar{\bar{I}} - \vec{R}^{(i)}) \cdot L (\vec{E}^{(i)}) \qquad (3.12)$$

where $L(\vec{E}^{(i)})$ is an operator abbreviation for the right hand side of equation (2.29).

Due to the limitations in precision on the Vax 11/750 computer in approximating derivatives Brand's results, using the contractor corrector scheme with the Newton-Raphson method, could not be duplicated. Therefore the secant method was used to assure convergence.

To accelerate the convergence and obtain an estimate of the error during each iteration, a new vector function was defined:

$$\vec{R}(\vec{E}) = L(\vec{E}) - \vec{E} \qquad (3.13)$$

$\vec{R}$ is called the residue vector and has a value proportional to the remaining error in the electric field. Using the secant method to find a new value for each field point utilized the following equation:

$$e^{(i+1)} = 1\{E^{(i)}, E^{(i-1)}\} = e^{(i)} - \frac{f\{E^{(i)}\}\{e^{(i)} - e^{(i-1)}\}}{f\{E^{(i)}\} - f\{E^{(i-1)}\}} \qquad (3.14)$$

In equation (3.14) 'e' represents the electric field at an individual cell point and 1 an individual element of the vector produced by the operator of equation (3.12).

IV. SOLUTION FOR CYLINDRICAL WAVES

In many antenna applications the source of the waves is considered to be in the far field of the antenna. This means that the wavefronts incident on the antenna can be approximated as planar. However in many dish type antennas (see Figure 6) the feeder is not in the far field, but in the near field of the antenna. The wavefronts will definitely have curvature characteristics of either cylindrical or spherical waves. This paper analyzes the scattering of cylindrical waves.

Cylindrical waves can be generated from a line source, such as in cylindrical antennas, or by impinging plane waves on the back of a flat opaque screen containing a long, very narrow slit. The latter technique is sometimes used in laser experiments. The geometry of a cylindrical wavefront is shown in Figure 7.

An equation for a cylindrical wave can be derived from the general three dimensional wave equation

$$\nabla^2 \Psi = {}^{1}/_{v^2} \, {}^{\partial^2 \Psi}/_{\partial t^2} \qquad (4.1)$$

using the cylindrical representation of the Laplacian operator

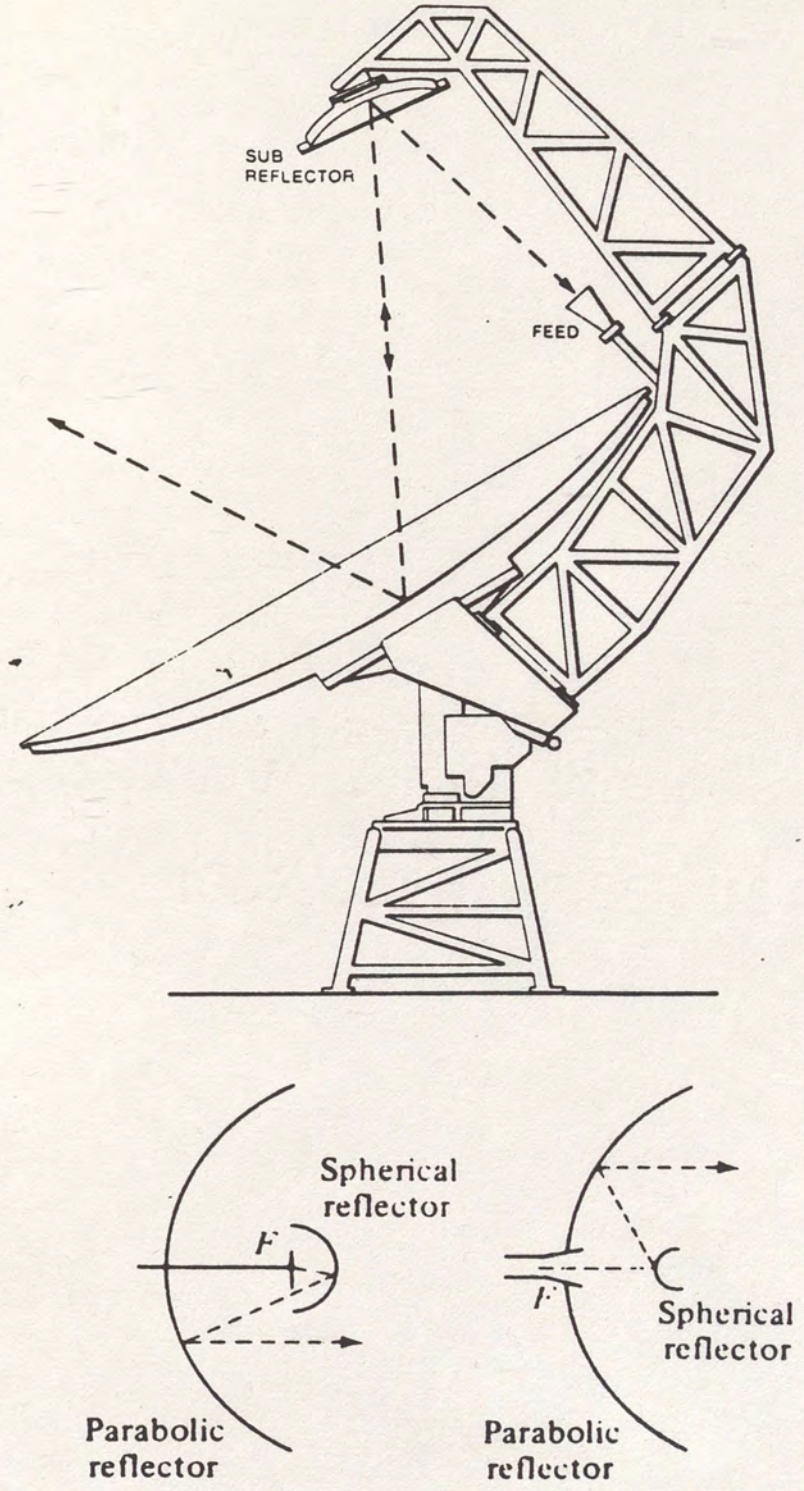

Figure 6. Reflecting Antennas.

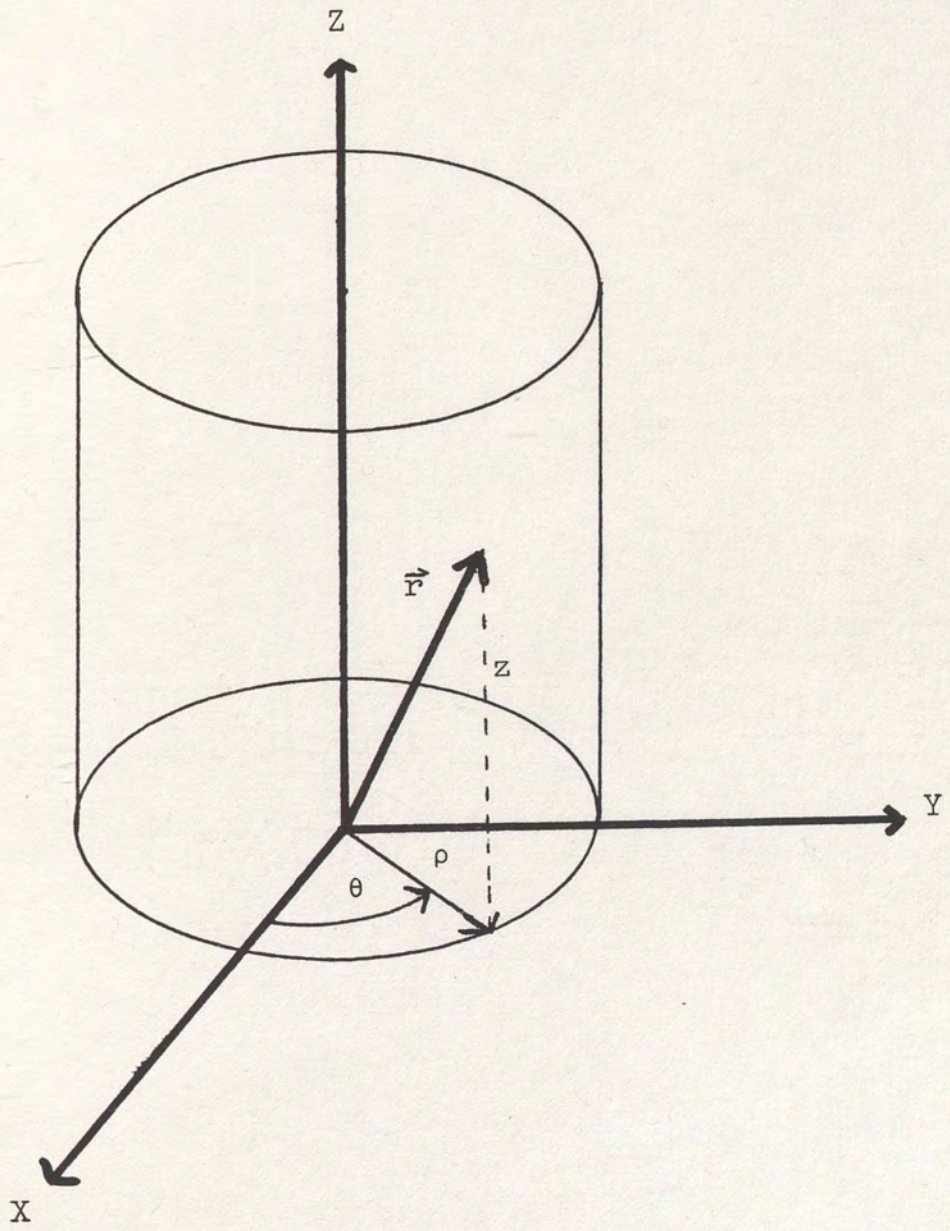

Figure 7. Cylindrical Coordinates.

$$\nabla^2\Psi = \frac{1}{r}\frac{\partial}{\partial r}\left(r\frac{\partial\Psi}{\partial r}\right) + \frac{1}{r^2}\frac{\partial\Psi^2}{\partial\Theta^2} + \frac{\partial\Psi^2}{\partial z^2} \qquad (4.2)$$

If an infinite right circular cylinder is considered then $\partial\Psi/\partial\Theta = 0$ and $\partial\Psi/\partial z = 0$ and the wave equation becomes:

$$\frac{1}{r}\frac{\partial}{\partial r}\left(r\frac{\partial\Psi}{\partial r}\right) = \frac{1}{v^2}\frac{\partial\Psi^2}{\partial t^2} \qquad (4.3)$$

The solution to the spatial part of equation (4.3) involves Bessel functions [12]. When r is sufficiently large we can approximate the solution as:

$$\Psi(r,t) = \{A/(r)^{1/2}\}\, e^{jk(r \pm vt)} \qquad (4.4)$$

This equation represents an infinite set of coaxial right circular cylinders filling all space and travelling radially outward or inward from an infinite line source (see Figure 8). Unlike the solution of the three dimensional wave equation in rectangular or spherical coordinates, there is no solution to the equation in cylindrical coordinates in terms of arbitrary functions [13].

To quantitatively analyze the scattering of cylindrical waves from a one dimensional planar structure the cylindrical wavefront is divided into N equal plane segments as shown in Figure 9. As N approaches infinity the connect planar segments approach a perfect cylindrical surface. Each

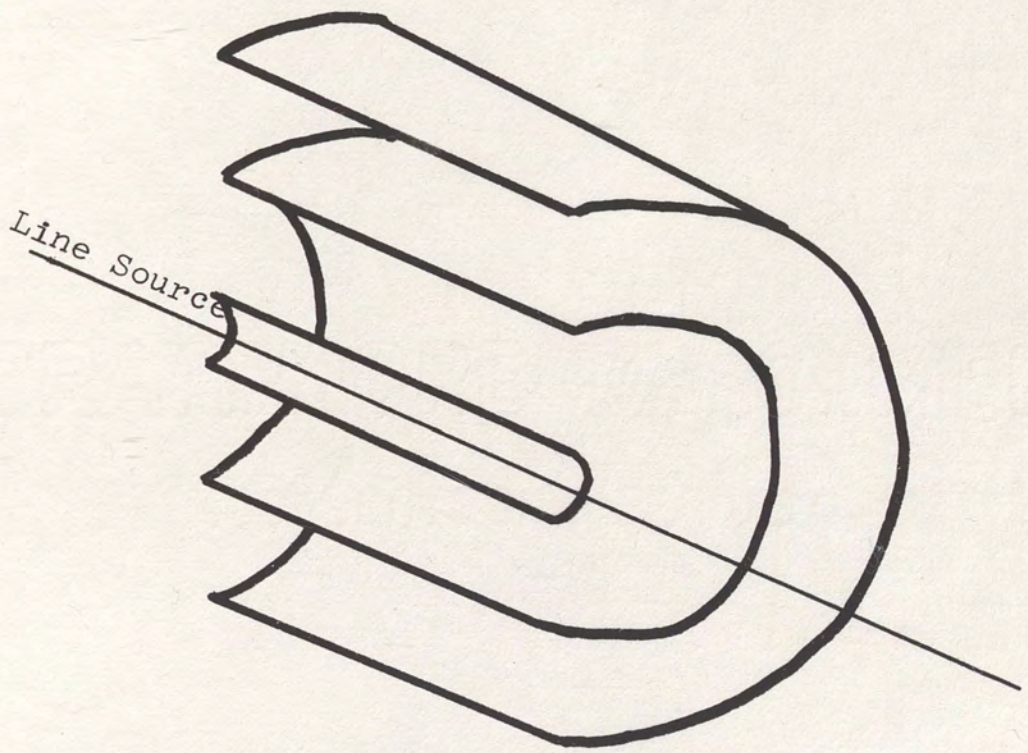

Figure 8. Cylindrical Waves.

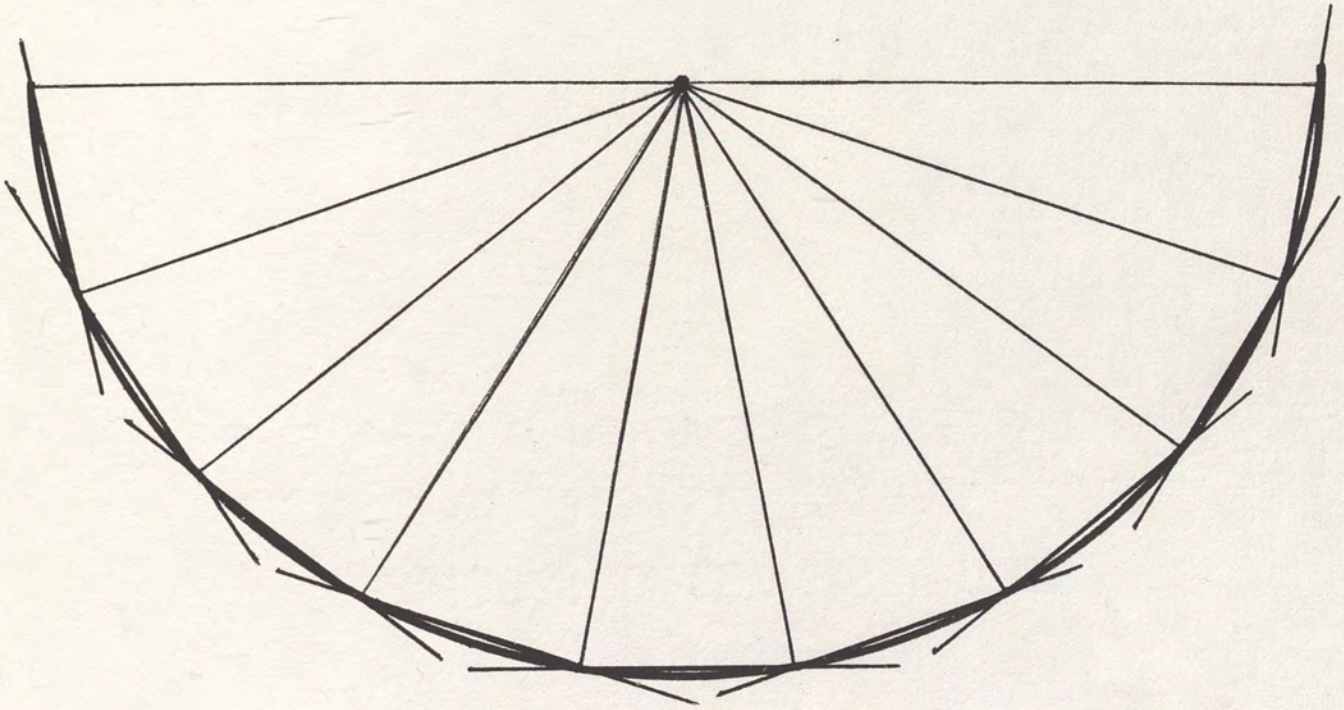

Figure 9. Segmented Cylindrical Wavefront.

planar segment is analyzed as if it were an infinite plane wave interacting with the wire array. The scattering parameters are then calculated using the SIT with the secant method to assure convergence.

The locally planar approximation of the cylindrical wavefront is analogous to recent work by Cwik and Mittra [14]. Instead of analyzing cylindrical waves incident on a planar one dimensional wire array, Cwik and Mittra analyzed the scattering of plane waves with wire strips arranged in cylindrical geometry (see Figure 10). They analyzed the scattering from each strip individually, to obtain a reflection coefficient, by assuming each strip was a member of an infinite one dimensional planar structure. The resulting reflection coefficient of the plane waves interacting with the cylindrical wire strip structure was calculated by combining the scattering parameters of the individual strips.

As can be seen in Figure 9, different regions on a cylindrical wavefront travel different distances in going from the source to the plane of the wire array. This is also true of the various plane segments when the cylindrical wavefront is divided into planar segments. Because of this, each plane wave has a different phase when interacting with each wire. The phase difference for each plane wave must be taken into consideration when calculating the reflection coefficient for the entire cylindrical wavefront.

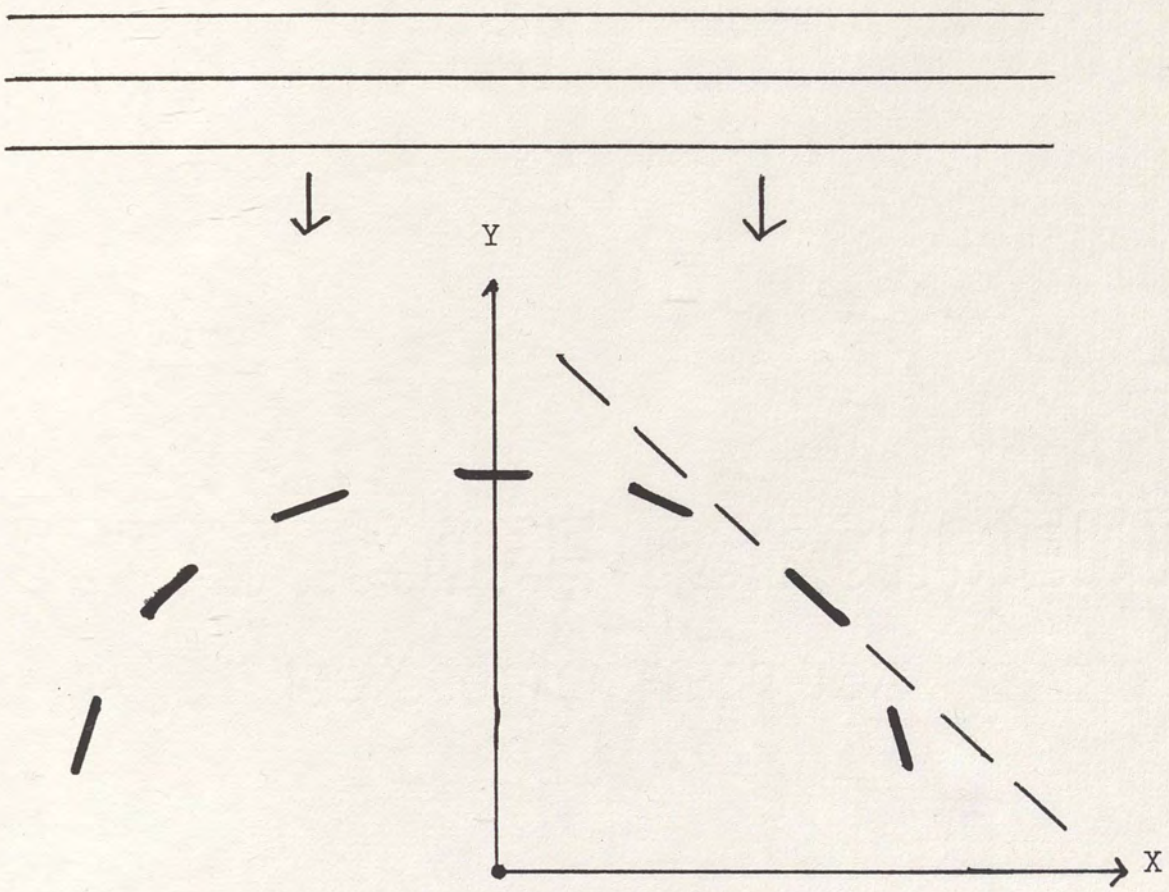

Figure 10. Locally Planar Approximation for Plane Waves Incident on a Cylindrical Wire Strip Structure.

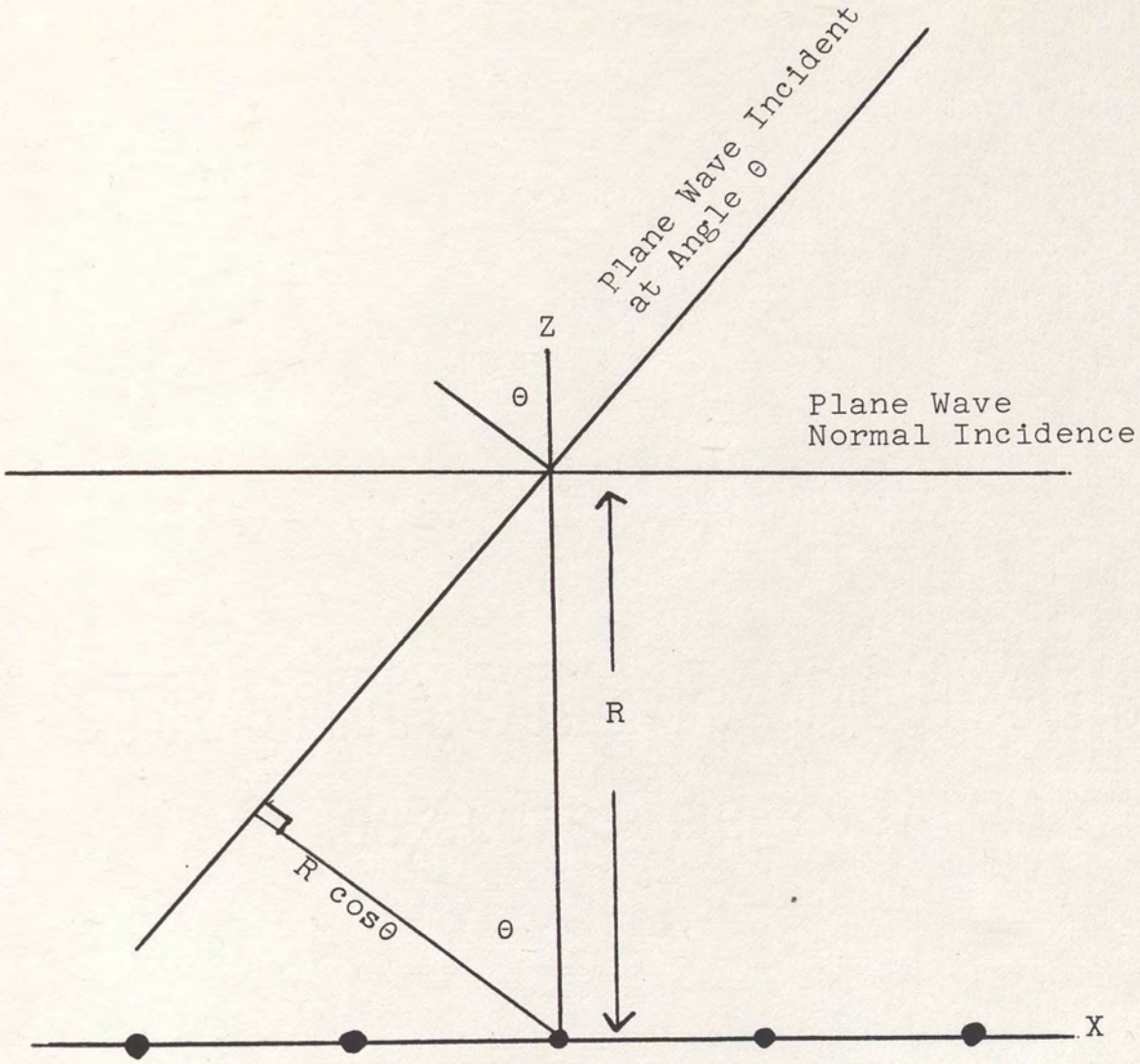

Figure 11. Geometry for Determination of Relative Phases of Plane Waves.

The additional distance travelled by a plane wave incident at angle Θ, in excess of the distance travelled by a normal plane wave, is illustrated in Figure 11. The path length difference is given by:

$$\Delta = R - R \cos \tag{4.5}$$

where R is the normal distance from the source to the wire array. If all dimensions are normalized to the wavelength of the radiation, then the phase difference between the normal incident plane wave and one incident at angle Θ is $2\pi\Delta$ or:

$$\Delta \text{ Phase} = 2\pi(R - R \cos\Theta) \tag{4.6}$$

RESULTS

The reflection coefficient is defined as the ratio of the power carried by the reflected wave to the power carried by the incident wave. The Fortran 77 program used to calculate reflection coefficients for plane waves incident on one dimensional, planar wire strips appears in Appendix A. The flowchart for the algorithm also appears in Appendix A. To perform the DFT called for in equation (2.29) a finite number of sampling points is required for a unit cell (see Figure 12). If an insufficient number of sampling points are chosen, large errors could result in the calculations. If too many sampling points are used the computation would take unnecessary extra time with no gain in accuracy. It was determined, from running a number of examples, that 32 sampling points per unit cell were sufficient to achieve accurate results.

The first results found in Tables 1 and 2 give the reflection coefficients for value of the angle θ from 0 to 90 degrees. In each, the cell width is 1/4 wavelengths, the wire diameter 1/600 wavelengths, the wire conductivity infinite and the frequency of the incident waves 3×10^8 Hz. When $\vec{E}$inc is parallel to the wires and $\phi = 0$ the Transverse Electric (TE) case arises, whereas when $\phi = 90$ degrees the Transverse Magnetic (TM) case arises.

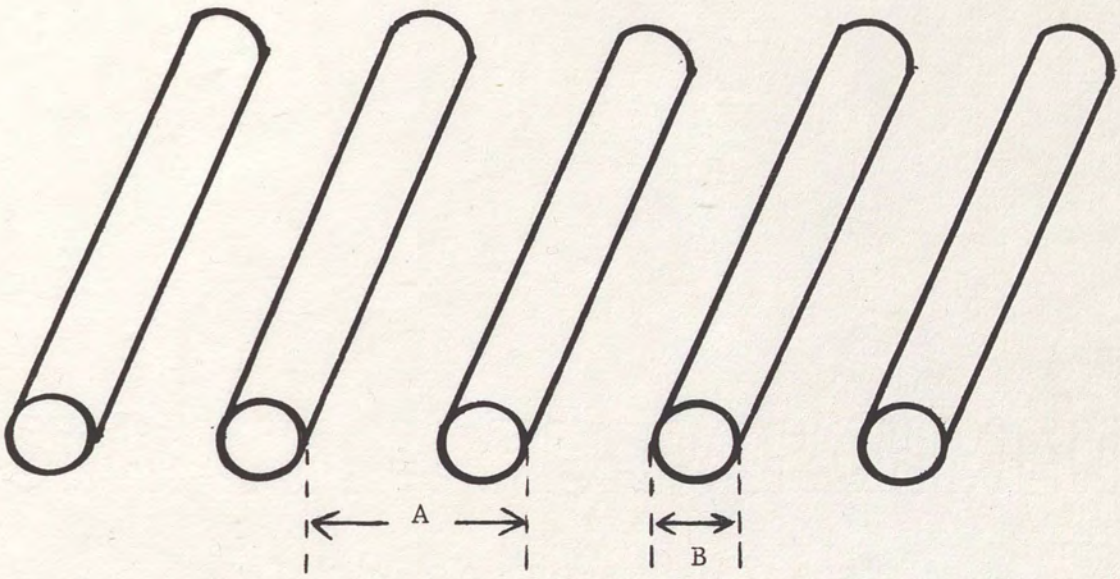

A = Cell width

B = Wire diameter

Figure 12. Unit Cell for a One Dimensional Wire Grating.

TABLE 1

REFLECTION COEFFICIENTS FOR PHI = 0 DEGREES

A=.25000 B=.0016700 TOL=.0001

I	ITER	THETA	REF	CREF
0	8	0.0000000E+00	0.5080711	(0.2581189,-0.4376196)
1	8	2.812500	0.5084996	(0.2585540,-0.4378603)
2	8	5.625000	0.5097930	(0.2598705,-0.4385844)
3	8	8.437500	0.5119604	(0.2620840,-0.4397902)
4	8	11.25000	0.5150177	(0.2652227,-0.4414749)
5	8	14.06250	0.5189862	(0.2693247,-0.4436336)
6	8	16.87500	0.5238938	(0.2744415,-0.4462584)
7	8	19.68750	0.5297757	(0.2806376,-0.4493382)
8	8	22.50000	0.5366731	(0.2879921,-0.4528560)
9	8	25.31250	0.5446340	(0.2965999,-0.4567874)
10	8	28.12500	0.5537136	(0.3065733,-0.4610981)
11	8	30.93750	0.5639727	(0.3180432,-0.4657400)
12	8	33.75000	0.5754787	(0.3311603,-0.4706469)
13	8	36.56250	0.5883038	(0.3460972,-0.4757290)
14	8	39.37500	0.6025254	(0.3630482,-0.4808668)
15	12	42.18750	0.6181175	(0.3820706,-0.4858922)
16	12	45.00000	0.6353867	(0.4037178,-0.4906407)
17	12	47.81250	0.6542955	(0.4281039,-0.4948027)
18	11	50.62500	0.6749089	(0.4554994,-0.4980183)
19	11	53.43750	0.6972721	(0.4861794,-0.4998179)
20	12	56.25000	0.7213826	(0.5203860,-0.4995911)
21	12	59.06250	0.7471794	(0.5582811,-0.4965877)
22	12	61.87500	0.7745454	(0.5999298,-0.4899029)
23	8	64.68750	0.8032299	(0.6453057,-0.4782874)
24	12	67.50000	0.8329148	(0.6937506,-0.4609308)
25	12	70.31250	0.8629787	(0.7447310,-0.4360136)
26	11	73.12500	0.8926740	(0.7968645,-0.4023353)
27	12	75.93750	0.9210050	(0.8482604,-0.3587541)
28	12	78.75000	0.9468177	(0.8964759,-0.3046221)
29	8	81.56250	0.9687710	(0.9385528,-0.2400747)
30	9	84.37500	0.9855854	(0.9715052,-0.1660009)
31	12	87.18750	0.99629541	(0.99267,-8.491265E-02)

TABLE 2

REFLECTION COEFFICIENTS FOR PHI = 90 DEGREES

A=.25000 B=.0016700 TOL=.0001

I	ITER	THETA	REF	CREF
0	8	0.0000000E+00	0.5080711	(0.2581189,-0.4376196)
1	8	2.812500	0.5303115	(0.2572254,-0.4637515)
2	8	5.625000	0.5536214	(0.2541778,-0.4918233)
3	8	8.437500	0.5773324	(0.2485401,-0.5210955)
4	10	11.25000	0.6006295	(0.2398987,-0.5506400)
5	10	14.06250	0.6230848	(0.2283397,-0.5797377)
6	10	16.87500	0.6438972	(0.2137750,-0.6073745)
7	10	19.68750	0.6623937	(0.1963854,-0.6326122)
8	10	22.50000	0.6779147	(0.1765237,-0.6545287)
9	10	25.31250	0.6898247	(0.1547047,-0.6722534)
10	10	28.12500	0.6975207	(0.1315964,-0.6849945)
11	10	30.93750	0.7004440	(0.1080038,-0.6920672)
12	10	33.75000	0.6980902	(8.485278E-02,-0.692914)
13	10	36.56250	0.6900250	(6.317369E-02,-0.687127)
14	10	39.37500	0.6759390	(4.405903E-02,-0.6745016)
15	8	42.18750	0.6557732	(2.8634697E-02,-0.655148)
16	8	45.00000	0.6291218	(1.799956E-02,-0.6288643)
17	8	47.81250	0.5963041	(1.330584E-02,-0.5961556)
18	8	50.62500	0.5577710	(1.561087E-02,-0.5575526)
19	8	53.43750	0.5144277	(2.5879726E-02,-0.513776)
20	8	56.25000	0.4678871	(4.495371E-02,-0.4657226)
21	8	59.06250	0.4209101	(7.352047E-02,-0.4144394)
22	8	61.87500	0.3781056	(0.112081,-0.3611117)
23	8	64.68750	0.3466377	(0.1609436,-0.3070095)
24	8	67.50000	0.3357515	(0.2201791,-0.2534764)
25	8	70.31250	0.3530512	(0.2896290,-0.2018915)
26	7	73.12500	0.3995559	(0.3688231,-0.1536700)
27	7	75.93750	0.4703254	(0.4572753,-0.1100240)
28	8	78.75000	0.5587655	(0.554068,-7.22998E-02)
29	6	81.56250	0.6592695	(0.6579555,-4.160386E-02)
30	6	84.37500	0.7681738	(0.7679435,-1.881126E-02)
31	6	87.18750	0.8824902	(0.8824774,-4.757401E-03)

For each plane wave segment convergence was determined when a new iteration did not produce a reflection coefficient different from the previous iteration in the fourth decimal place (TOL=0.0001). In Tables 1 and 2 it is shown each set of data converged within 8-12 iterations. The data under the column labeled "CREF" is the complex reflection coefficient whose magnitude yields the reflection coefficient to the left.

Tables 3 and 4 show the same data as in Tables 1 and 2, respectively, except in calculating this data TOL=0.000005 was used. For most of the various angles of incidence convergence occurred between 12-16 iterations. The data show that the additional iterations do not change the values of the complex and actual reflection coefficients to the fourth significant figure.

The data from Tables 1 and 2 are plotted in Figure 13 and 14, respectively, along with data from Brand for comparison. The plots give the reflection coefficients versus angle of incidents for either TE (Figure 13) or TM (Figure 14) plane waves. The data are in good agreement with that of Brand's. For both polarizations the reflection coefficients approach unity as θ approaches 90 degrees, as would be expected. In Figure 14 the minimum at θ =67 degrees is due to an effect similar to the Brewster angle associated with dielectric materials.

TABLE 3

REFLECTION COEFFICIENTS FOR PHI = 0 DEGREES

A= .25000 B= .00167000 TOL = .000005

I	ITER	THETA	REF	CREF
0	12	0.0000000E+00	0.5080244	(0.2580888,-0.4375831)
1	12	2.812500	0.5084522	(0.2585237,-0.4378231)
2	12	5.625000	0.5097442	(0.2598394,-0.4385460)
3	12	8.437500	0.5119097	(0.2620518,-0.4397503)
4	12	11.25000	0.5149640	(0.2651884,-0.4414330)
5	12	14.06250	0.5189290	(0.2692872,-0.4435896)
6	12	16.87500	0.5238317	(0.2743986,-0.4462119)
7	12	19.68750	0.5297066	(0.2805882,-0.4492877)
8	12	22.50000	0.5365964	(0.2879350,-0.4528014)
9	12	25.31250	0.5445492	(0.2965333,-0.4567294)
10	12	28.12500	0.5536197	(0.3064945,-0.4610378)
11	12	30.93750	0.5638699	(0.3179494,-0.4656795)
12	12	33.75000	0.5753685	(0.3310492,-0.4705904)
13	12	36.56250	0.5881896	(0.3459677,-0.4756820)
14	12	39.37500	0.6024120	(0.3629013,-0.4808356)
15	12	42.18750	0.6181175	(0.3820706,-0.4858922)
16	12	45.00000	0.6353867	(0.4037178,-0.4906407)
17	12	47.81250	0.6542955	(0.4281039,-0.4948027)
18	13	50.62500	0.6749132	(0.4555050,-0.4980192)
19	12	53.43750	0.6972702	(0.4861781,-0.4998164)
20	16	56.25000	0.7213715	(0.5203763,-0.4995853)
21	16	59.06250	0.7471775	(0.5582729,-0.4965940)
22	16	61.87500	0.7745508	(0.5999291,-0.4899123)
23	15	64.68750	0.8032594	(0.6452252,-0.4784455)
24	16	67.50000	0.8329225	(0.6937591,-0.4609317)
25	16	70.31250	0.8629803	(0.7447366,-0.4360074)
26	11	73.12500	0.8926740	(0.7968645,-0.4023353)
27	28	75.93750	0.9210095	(0.8482622,-0.3587614)
28	20	78.75000	0.9468343	(0.8964922,-0.3046259)
29	12	81.56250	0.9688268	(0.9386266,-0.2400113)
30	51	84.37500	0.9857143	(0.9716344,-0.1660090)
31	38	87.18750	0.9963639	(0.992737,-8.493589E-02)

TABLE 4

REFLECTION COEFFICIENTS FOR PHI = 90 DEGREES

A= .250000 B= .00167000 TOL= .000005

I	ITER	THETA	REF	CREF
0	12	0.0000000E+00	0.5080244	(0.2580888,-0.4375831)
1	12	2.812500	0.5302564	(0.2571883,-0.4637090)
2	12	5.625000	0.5535581	(0.2541341,-0.4917748)
3	12	8.437500	0.5772617	(0.2484903,-0.5210410)
4	12	11.25000	0.6006877	(0.2399605,-0.5506766)
5	12	14.06250	0.6231506	(0.2283996,-0.5797847)
6	12	16.87500	0.6439663	(0.2138270,-0.6074296)
7	12	19.68750	0.6624615	(0.1964298,-0.6326694)
8	12	22.50000	0.6779778	(0.1765614,-0.6545838)
9	12	25.31250	0.6898815	(0.1547376,-0.6723042)
10	12	28.12500	0.6975727	(0.1316266,-0.6850416)
11	12	30.93750	0.7004933	(0.1080336,-0.6921124)
12	12	33.75000	0.6981439	(8.488294E-02,-0.692965)
13	12	36.56250	0.6900975	(6.319419E-02,-0.687198)
14	12	39.37500	0.6760153	(4.405713E-02,-0.674578)
15	15	42.18750	0.6556798	(2.860594E-02,-0.6550566)
16	14	45.00000	0.6290373	(1.797250E-02,-0.628780)
17	16	47.81250	0.5962260	(1.328898E-02,-0.596078)
18	14	50.62500	0.5577026	(1.560462E-02,-0.557484)
19	15	53.43750	0.5143835	(2.587208E-02,-0.513732)
20	13	56.25000	0.4678625	(4.494757E-02,-0.465698)
21	12	59.06250	0.4208988	(7.351937E-02,-0.414428)
22	12	61.87500	0.3781001	(0.112088,-0.3611038)
23	11	64.68750	0.3466374	(0.1609533,-0.3070041)
24	9	67.50000	0.3357523	(0.2201900,-0.2534679)
25	10	70.31250	0.3530590	(0.2896369,-0.2018938)
26	9	73.12500	0.3996142	(0.3689017,-0.1536329)
27	9	75.93750	0.4703794	(0.4573304,-0.1100259)
28	9	78.75000	0.5587636	(0.554066,-7.230312E-02)
29	8	81.56250	0.6593485	(0.658036,-4.157845E-02)
30	8	84.37500	0.7682067	(0.767976,-1.881057E-02)
31	7	87.18750	0.8824912	(0.882478,-4.766003E-03)

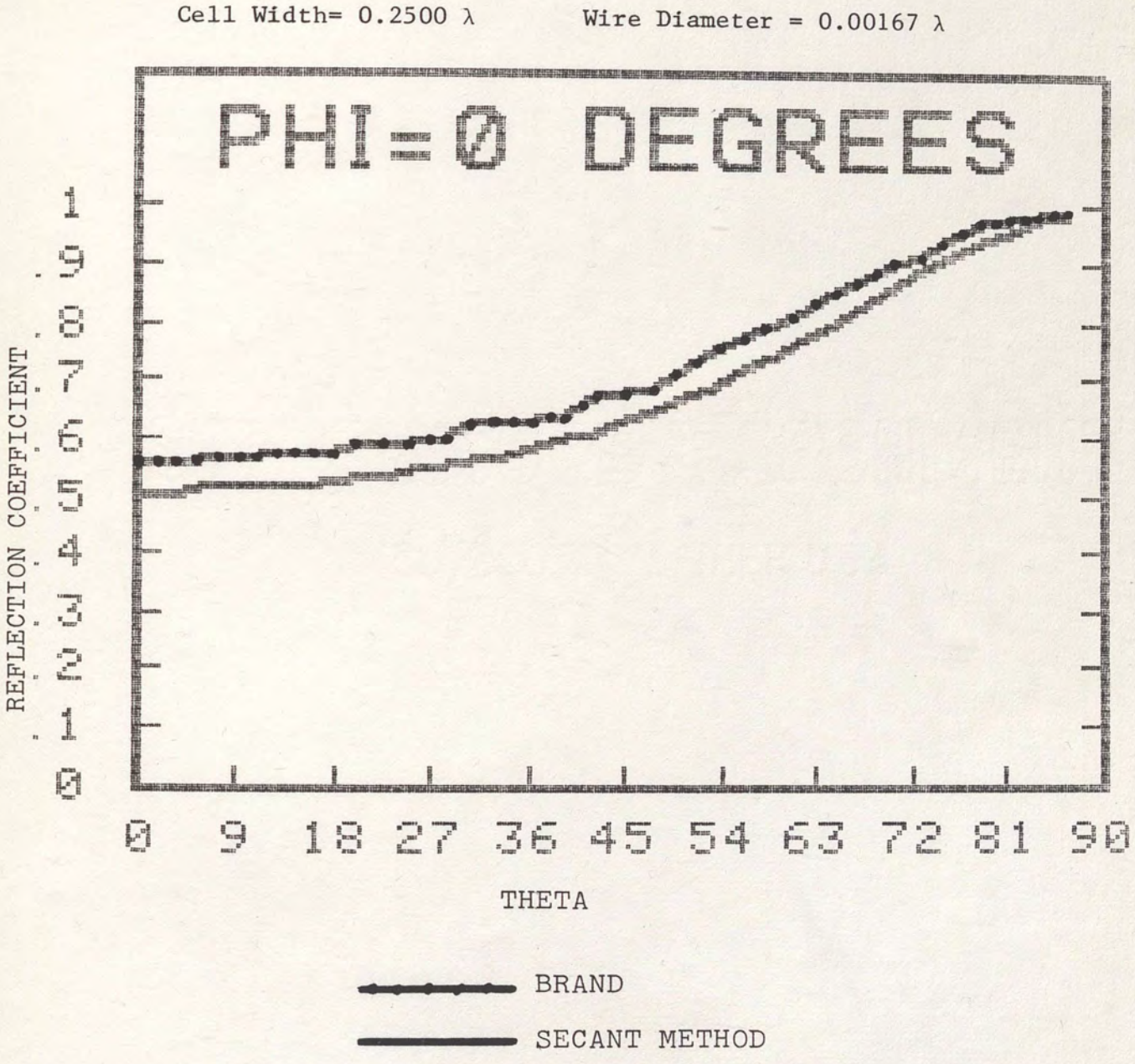

Figure 13 Reflection Coefficients for TE Plane Waves

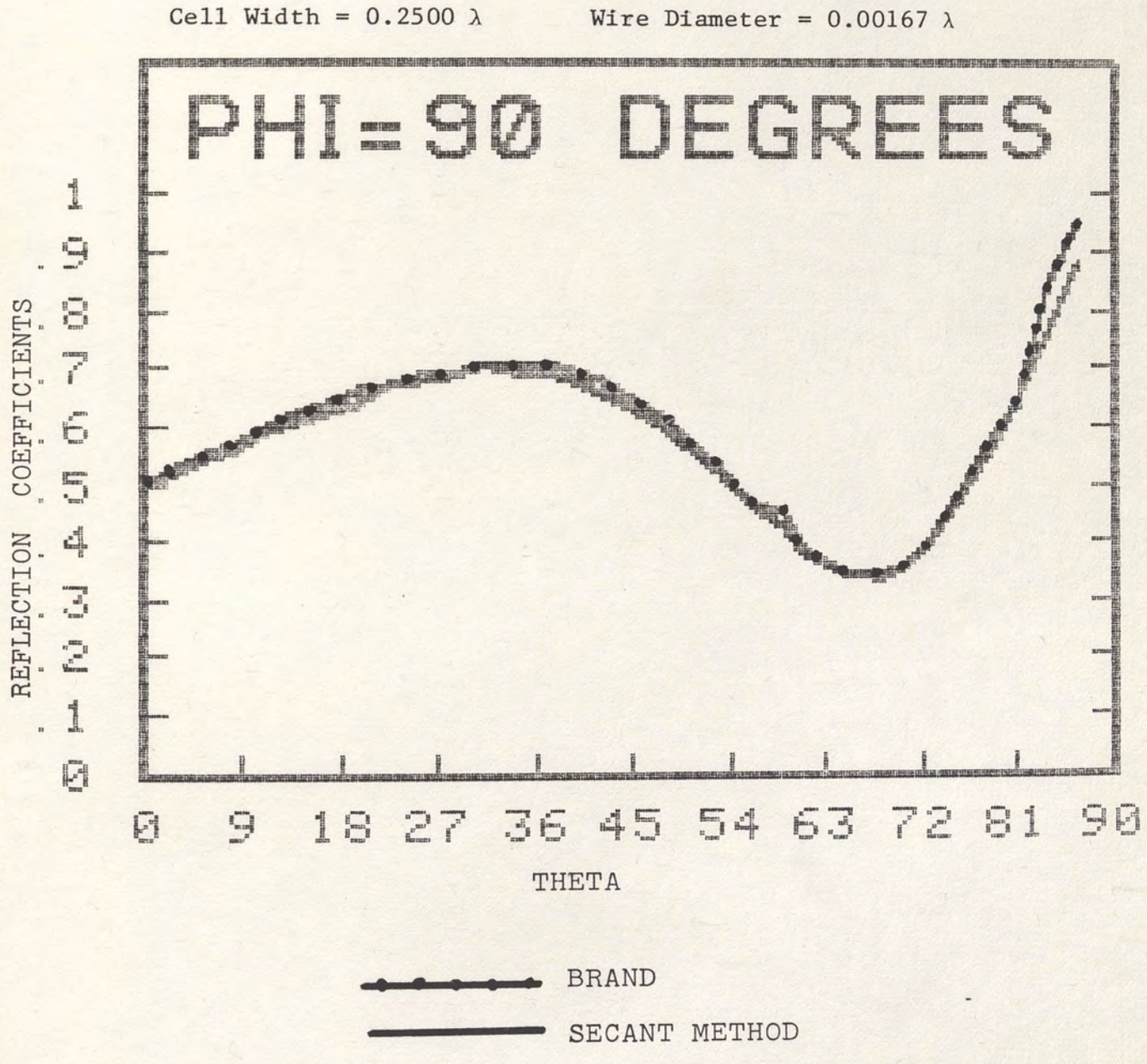

Figure 14 Reflection Coefficients for TM Plane Waves

The values of the reflection coefficients shown in Tables 1-4 are independent of the phase of the plane waves when interacting with the wire grids. The phase of each plane wave, regardless of the angle of incidence, was chosen to be zero for simplicity in the calculation. If non-zero phases were used the complex reflection coefficients would have different real and imaginary contributions but their magnitudes (complex absolute values) would agree with Tables 1 and 2.

As discussed at the end of the previous chapter, when a cylindrical wavefront is approximated with N equal planar segments the phase of each plane wave will be different upon reaching the same unit cell. The phase difference for each planar segment was incorporated into the calculation of the reflection complex coefficient for each segment. The complex reflection coefficients for all N segments composing the cylindrical wavefront were then summed, the summation accounting for the interference of the plane waves resulting in the scattered field. The magnitude of this summation yields the reflection coefficient of the cylindrical wavefront.

Data in Tables 5, 6, and 7 investigate the affects of increasing the cell width (A), the wire diameter (B) and the number of divisions in the cylindrical wavefront (N). In Table 5 the cell width is varied from 1/20 to 1 wavelength, using 1 meter as the wavelength. The wire diameter is 1/600

TABLE 5

EFFECT OF VARYING CELL SIZE ON REFLECTION COEFFICIENTS

B=.0016700 FREQ = 3×10^8

CELL WIDTH NORMALIZED IN WAVELENGTHS	REFL COEF 15 SEGMENTS	REFL COEF 63 SEGMENTS	REFL COEF 255 SEGMENTS
0.05	0.2325552	0.0847749	0.0889166
0.10	0.1909643	0.0682722	0.0782886
0.15	0.1690416	0.0554957	0.0674766
0.20	0.1589005	0.0449779	0.0574633
0.25	0.1550571	0.0365062	0.0507194
0.30	0.1531066	0.0299295	0.0445608
0.35	0.1506540	0.0248589	0.0397931
0.40	0.1464682	0.0208146	0.0360254
0.45	0.1385338	0.0174191	0.0329772
0.50	0.1020095	0.0300464	0.0389571
0.55	0.0867519	0.0144412	0.0271213
0.60	0.1222615	0.0168553	0.0305144
0.65	0.1352660	0.0147346	0.0292187
0.70	0.1226075	0.0020271	0.0178167
0.75	0.1226082	0.0154404	0.0278441
0.80	0.1104891	0.0148839	0.0212141
0.85	0.0990582	0.0099615	0.0125863
0.90	0.1003822	0.0066987	0.0101432
0.95	0.0941252	0.0047959	0.0122554
1.00	0.0704742	0.0193412	0.0113168

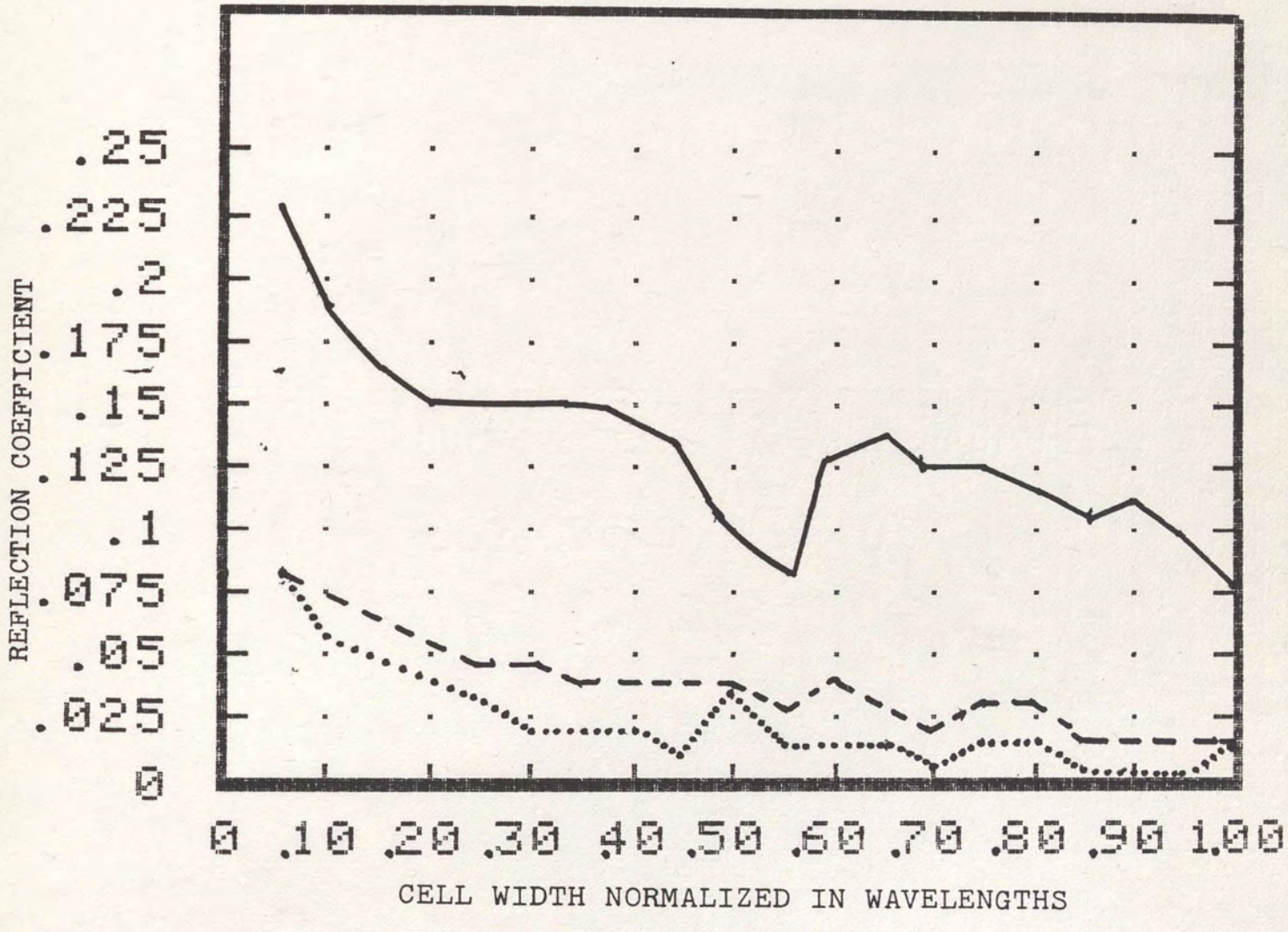

Figure 15 Reflection Coefficient vs. Cell Width for Wire Diameter = .00167 Wavelengths

wavelength and the TE waves are emitted from a line source 10 wavelengths from the plane of the array. The reflection coefficients are given for cylindrical wavefronts by approximating the wavefronts with 15, 63 and then 255 equal segments, respectively. The data in Table 5 is plotted in Figure 15.

It can be seen from Table 5 or Figure 15 that as the cell width increases the reflection coefficients decrease. This is expected since as the cell size increases the density of the conducting material in the plane of the array decreases. As the number of planar segments used to approximate the cylindrical wavefront increase from 15 to 63 the reflection coefficients for a given cell size decreases. This is because when the wavefront is divided into 63 plane segments there is more destructive interference than with 15 segments. The effect of interference seems to converge as N is increased further as a slight increase in reflection coefficient for each cell width is seen when N goes from 63 to 255. It is assumed the data for N=255 approximate closely the data that would be obtained if N was infinite, i.e. a perfect cylindrical wavefront.

Table 6 shows data that was calculated with only one parameter different than than in Table 5. The wire diameter used for the data in Table 6 is 1/25 wavelength which is an increase of a factor of 24. The data in Table 6 is plotted in Figure 16.

TABLE 6

EFFECT OF VARYING CELL SIZE ON REFLECTION COEFFICEINTS

B=0.04000 FREQ = $3X10^8$

CELL WIDTH NORMALIZED IN WAVELENGTHS	REFL COEF 15 SEGMENTS	REFL COEF 63 SEGMENTS	REFL COEF 255 SEGMENTS
0.05	0.2549329	0.09132759	0.09149617
0.10	0.2464367	0.08962220	0.09127969
0.15	0.2308726	0.08511704	0.08937640
0.20	0.2107107	0.07768848	0.08475764
0.25	0.1920648	0.06932328	0.07861032
0.30	0.1747310	0.05902413	0.07031036
0.35	0.1630703	0.04753717	0.06064297
0.40	0.1607334	0.04199014	0.05558897
0.45	0.1544519	0.03137307	0.04629293
0.50	0.1298209	0.03772403	0.07266707
0.55	0.0861683	0.02436480	0.03876685
0.60	0.1237208	0.02700567	0.04128870
0.65	0.1468876	0.01981657	0.03476476
0.70	0.1340668	0.00398165	0.02091228
0.75	0.1365446	0.02027389	0.03347616
0.80	0.1220749	0.01807635	0.00914560
0.85	0.1078224	0.01098275	0.01382890
0.90	0.1121742	0.00662250	0.02403339
0.95	0.1076370	0.00449070	0.01224352
1.00	0.0894236	0.00978884	0.02085624

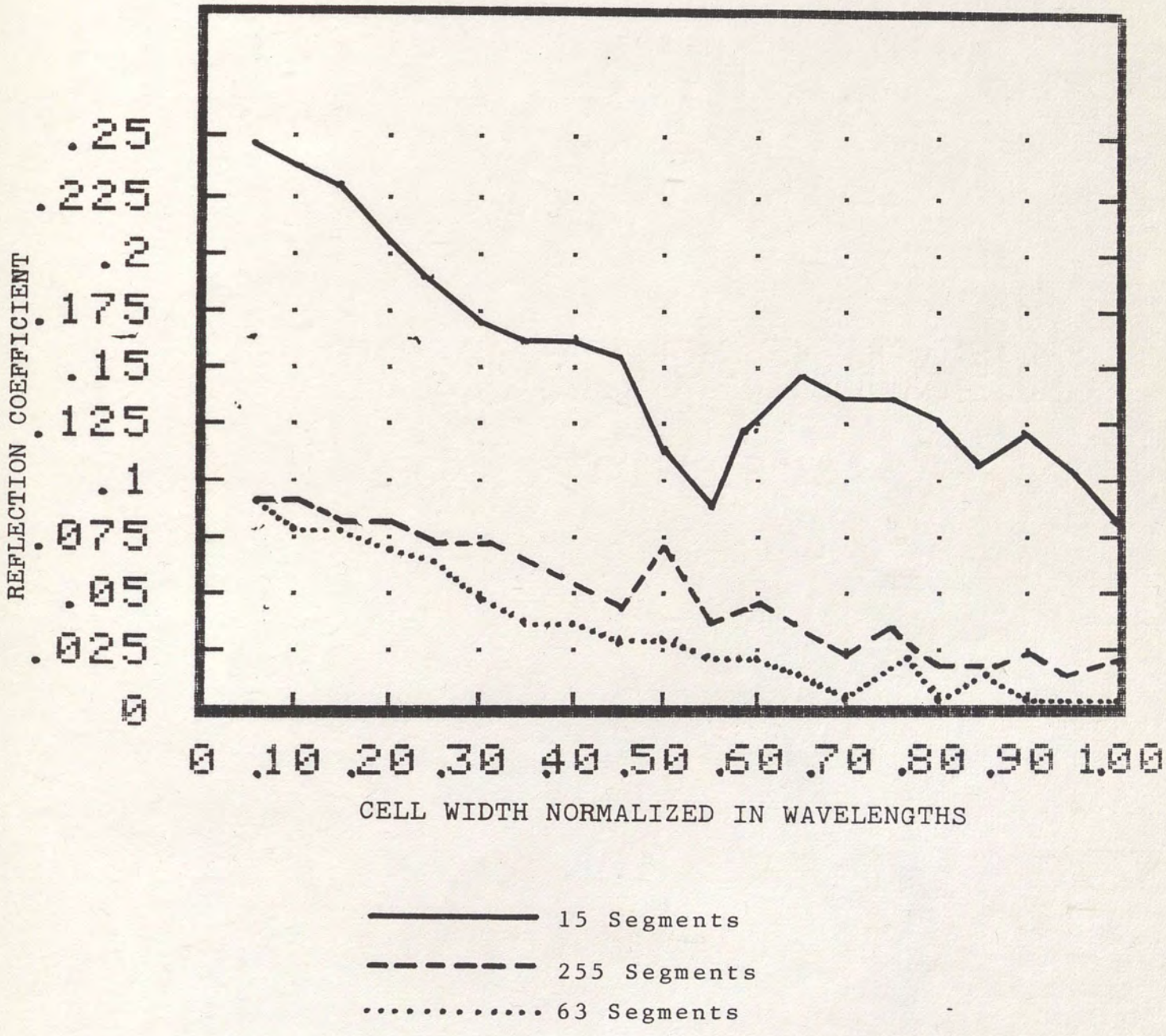

Figure 16 Reflection Coefficient vs. Cell Width for Wire Diameter = .04 Wavelengths

As can be seen in Figure 16 the trends of increasing N and increasing the cell width are the same as discussed above for the smaller wire diameter. The effect of increasing the wire diameter resulted in larger reflection coefficients. The increase in reflection coefficients is most readily seen when the cell size is smaller because the wire diameter is a larger and a more appreciable fraction of the entire cell width. As the cell width approaches 1 wavelength the effect of a wire diameter of 1/25 verses 1/600 is negligible because both of these diameters result in only 1 sampling point, of the 32 per unit cell used in the DFT, lying on the conductor.

Finally, in Table 7 data is shown with the same parameters as in the previous two tables except the wire diameter is increased each time the cell width is increased maintaining a wire diameter to cell width ratio of 1:2. The data from Table 7 is plotted in Figure 17.

As expected the reflection coefficients do not decrease as much with increasing cell size as when the cell size was increased with fixed wire diameters. However the reflection coefficients are still decreasing as the wire spacing increases, even with maintaining the wire diameter cell width ratio constant, since as the cell width increases the density of the conducting regions on in the plane of the array is still decreasing.

TABLE 7

EFFECT OF VARYING CELL SIZE WITH A FIXED CELL WIDTH TO WIRE DIAMETER RATIO

B=0.5 A FREQ = $3X10^8$

CELL WIDTH NORMALIZED IN WAVELENGTHS	REFL COEF 15 SEGMENTS	REFL COEF 63 SEGMENTS	REFL COEF 255 SEGMENTS
0.05	0.2525846	0.0908471	0.0914464
0.10	0.2493727	0.0901349	0.0914761
0.15	0.2461715	0.0894191	0.0912976
0.20	0.2426991	0.0885736	0.0910743
0.25	0.2389251	0.0875042	0.0907436
0.30	0.2350405	0.0864553	0.0901316
0.35	0.2311909	0.0850918	0.0894236
0.40	0.2266577	0.0835397	0.0885369
0.45	0.2222541	0.0818765	0.0875621
0.50	0.2165210	0.0791452	0.0859971
0.55	0.2113463	0.0783896	0.0851149
0.60	0.1876374	0.0763665	0.0822011
0.65	0.1810414	0.0740422	0.0792960
0.70	0.1814635	0.0656511	0.0760733
0.75	0.1897518	0.0710045	0.0929670
0.80	0.1934909	0.0689960	0.0800347
0.85	0.1785723	0.0542438	0.0671886
0.90	0.1668677	0.0384986	0.0516680
0.95	0.1565323	0.0254936	0.0680036
1.00	0.1406198	0.0197900	0.0322063

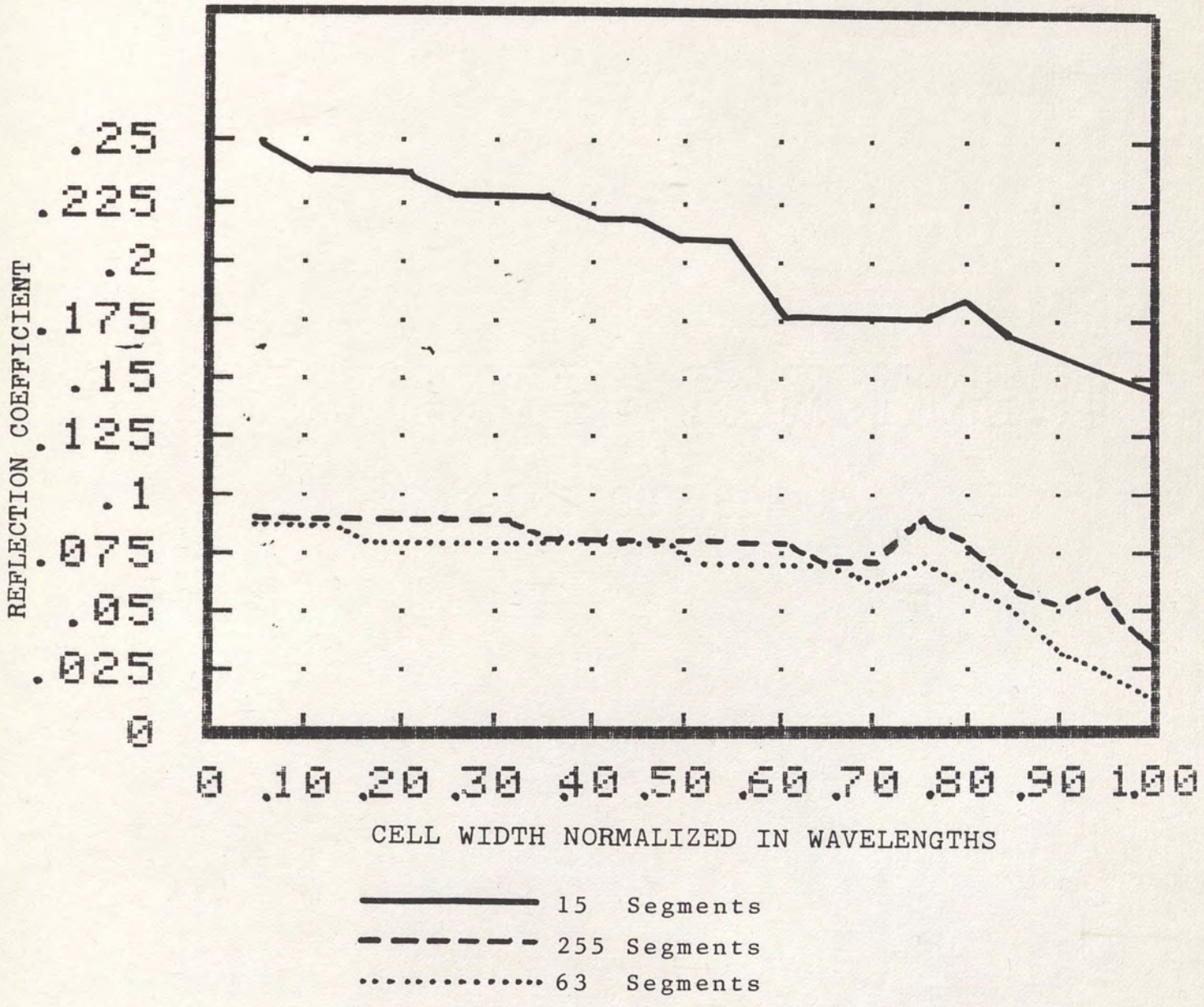

Figure 17 Reflection Coefficient vs. Cell Width with a Fixed Wire Diameter to Cell Width Ratio

VI. Summary, Conclusions and Recommendations

When a cylindrical wavefront is approximated by planar segments, the calculation of the scattering parameters can be accomplished through well established numerical techniques. The secant method can be used to solved an iterative scheme for the solutions of the fields and currents when infinite plane waves are incident on planar wire gratings. The secant method does not have the computational problems encounted with the Newton-Raphson method since calculations of numerical derivatives are not necessary.

It has been shown that the reflection coefficients for cylindricl waves are less than those for plane waves incident upon identical wire gratings. This is because of the interference that occurs as different segments of the incident wavefront scatter from the wire grating. Since no previous calculations could be found in the literature for cylindrical waves scattering with one dimensional planar wire gratings, there was no data for comparison. However, the reflection coefficients calculated are of the same magnitude as those calculated by Cwik and Mittra for scattering of plane waves with wire strips arranged on the surface of a cylinder [14].

It was found that the reflection coefficients for cylindrical waves decrease as the wire spacing increases. Since the cell width and source distance were both normalized in wavelengths there was only one independent variable of the three. Also the grating was assumed to be infinite. Therefore decreasing the wavelength holding the cell width and source distance constant, or decreasing the source distance holding the wavelength and cell width constant both would have the same affect as increasing the cell width holding the wavelength and source distance constant. Only the latter was investigated.

The spectral iteration method has not previously been applied to geometries other than plane waves incident on planar wire arrays. Scattering of cylindrical waves on wire structures with finite conductivities should be investigated as well as scattering with wires perpendicular or skewed to the one dimensional grating presented here. If the locally planar approximation is valid for cylindrical waves it should also be valid for spherical waves. The division of spherical wavefronts into planar segments would be more difficult than cylindrical waves but the algorithms exist for the analysis of the scattering of each planar segment.

APPENDIX A

Flowcharts, Subroutines and Main Program

The following program is written in Fortran 77 and was run on a Vax 11/750. The program prompts for data inputs from the unit cell, the source distance , the number of planar segments into which the wavefront is divided, and the frequency of the incident cylindrical waves. Prior to the listing of the program are listings of the program variables and flowcharts

Program Variables

E(I)	Electric field in aperture
Guess(I)	Previous estimate of the electric field
FI(I)	Current value of the residue function
FIM1(I)	Previous value of the residue function
G(I)	Transformed Green's Function
EINC	Incident electric field
HI	Incident magnetic field
CREF(ITH)	Complex reflection coefficient
REF(ITH)	Magnitude of complex reflection coefficient
CONVERGED	Boolean indicator of convergence
K	Propagation constant
CK	Constants used in iterative equations
MAX	Number of sampling points
ITER	Running count of number of iterations
CYCLES	Maximum number of iterations allowed
ITH	Index for planar segments
ALPHA	Phase of each planar segment
RADIUS	Source distance from grating
JC(I)	Current density across aperture

Other variable and constants are self explanatory and are not defined.

Subroutines and Functions

SINHH	Complex hyperbolic sine function
COSHH	Complex hyperbolic cosine function
FNCTZ	The residue vector
XFORM	Original transformation for electric field
FFT	Fast Fourier Transform
TRCOPR	Truncation function
TRCOPRC	Complimentary truncation function

FLOW CHART

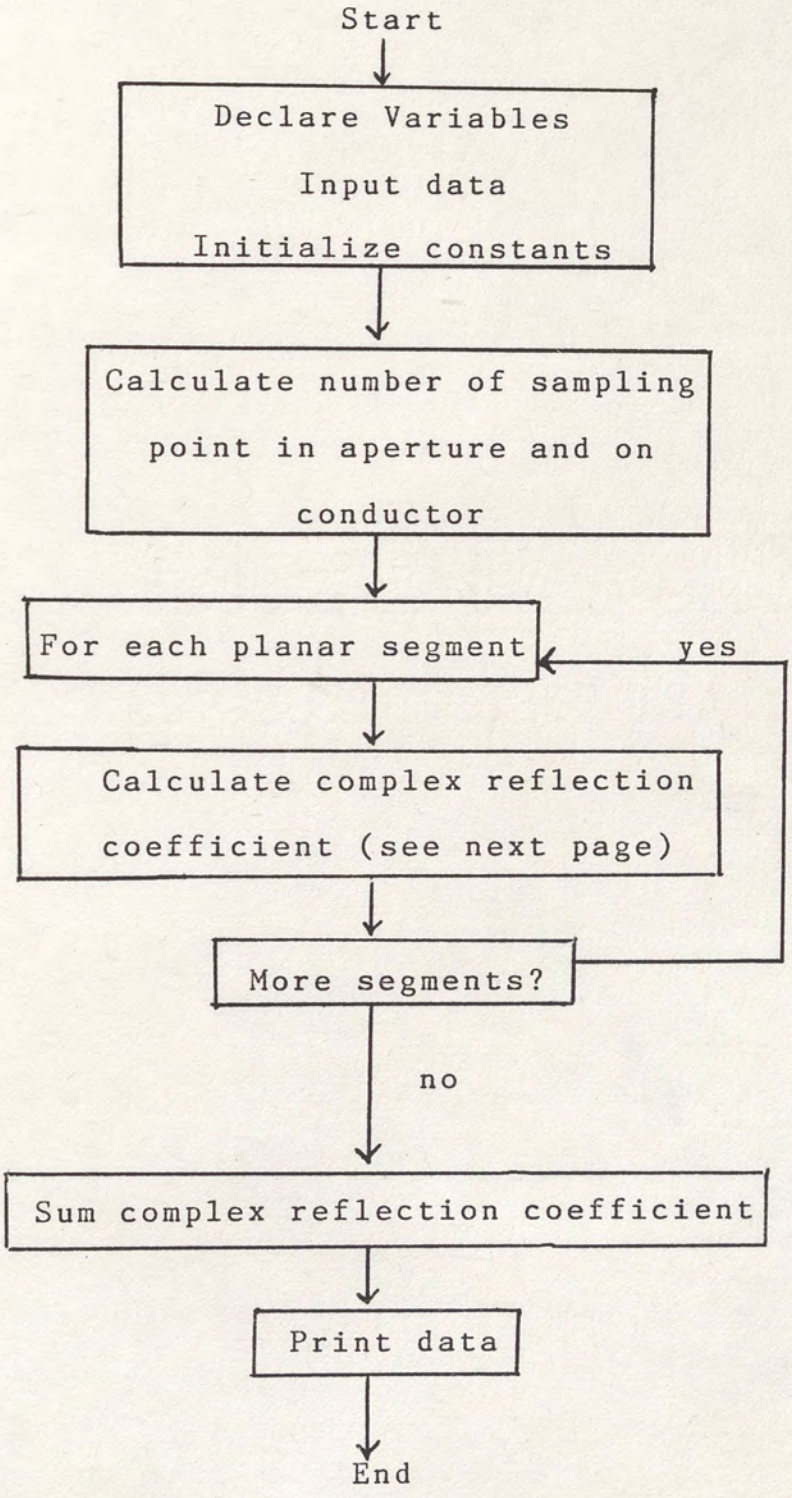
Start
Declare Variables
Input data
Initialize constants
Calculate number of sampling point in aperture and on conductor
For each planar segment
yes
Calculate complex reflection coefficient (see next page)
More segments?
no
Sum complex reflection coefficient
Print data
End

For each planar segment calculation of the complex reflection coefficient goes as follows

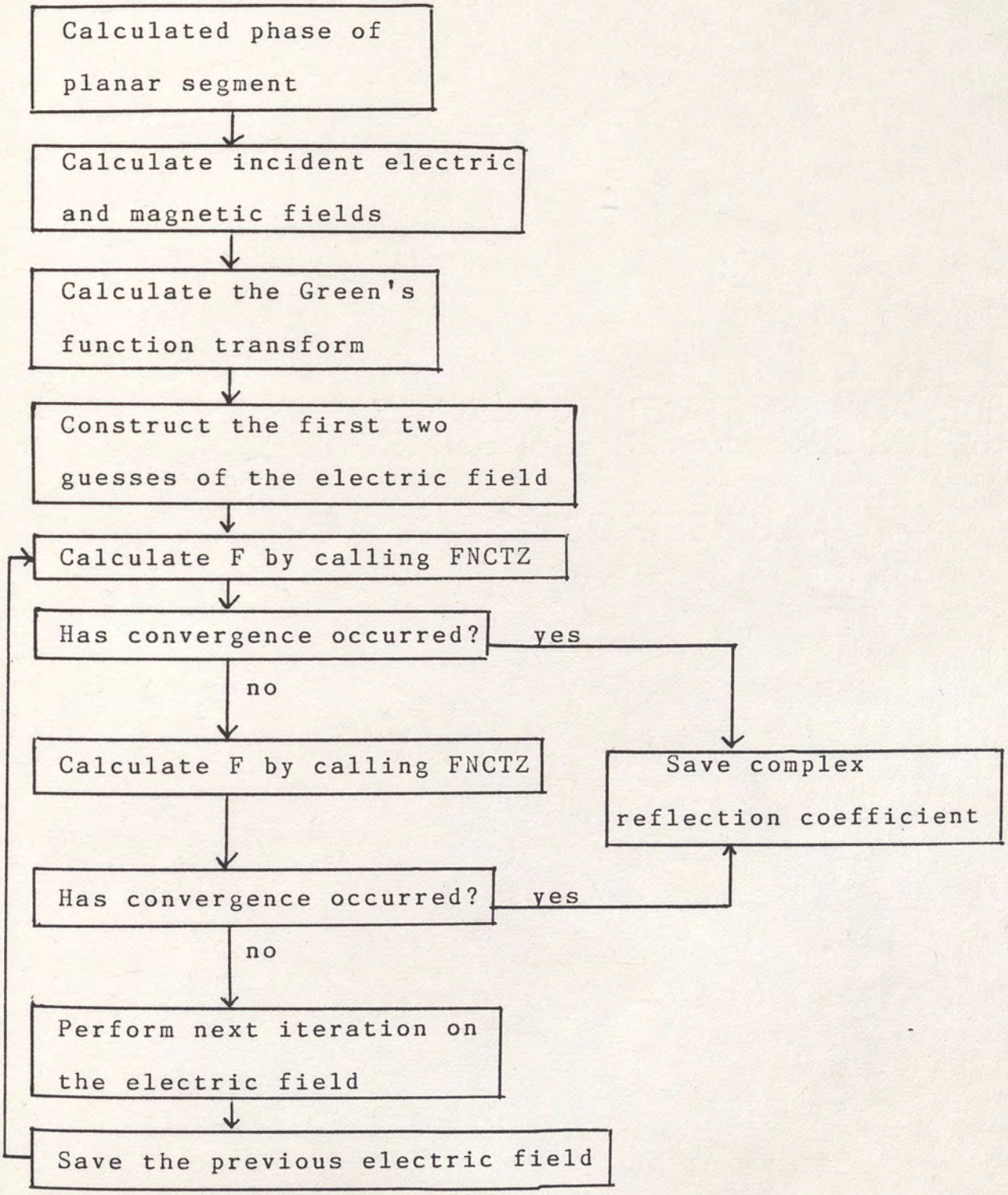

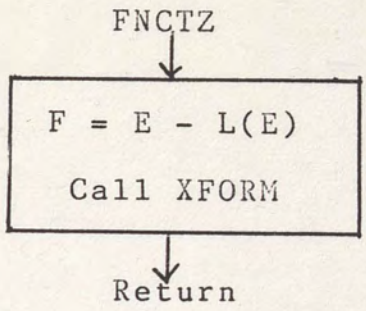
FNCTZ
F = E - L(E)
Call XFORM
Return

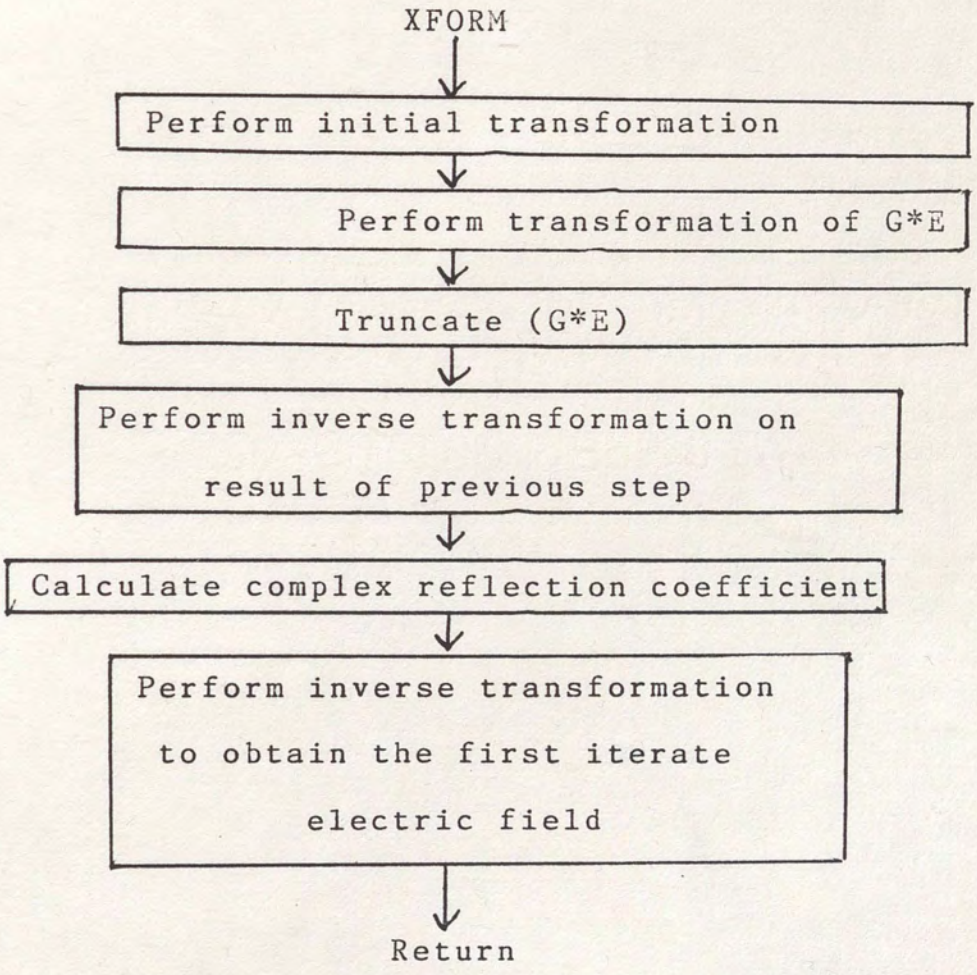
XFORM
Perform initial transformation
Perform transformation of G*E
Truncate (G*E)
Perform inverse transformation on result of previous step
Calculate complex reflection coefficient
Perform inverse transformation to obtain the first iterate electric field
Return

LISTING OF PROGRAM

```
C THIS FILE COPY FOR JAMES R DIRE
C**********************CYLEQSEG.FOR**********************
***** C SECANT METHOD APPLIED TO ASSURE CONVERGENCE
C
C
C
C DIMENSION ALL ARRAYS
      COMPLEX E(32),FI(32),FIM1(32),JC(32),G(32)
      COMPLEX RI,CREF,HI,EHOLD(32)
      COMPLEX GUESS(32),COMPREF,CRF,EINC
      COMPLEX J,CK1(32),CK2(32),CK(32),Z,T1,SINHH,COSHH
      REAL K,K2,RS1,RS2,SKIND1,RATIO
      INTEGER ITER,CYCLES
      LOGICAL CONVERGED
      COMMON RI,CREF(1025),HI,EINC
      COMMON JC,G,J,Z,CK
      COMMON
N,N1,IW,MAX,W,UU,STH,DR,REF(1025),ITH,ITHETA,B,ITER
C A = FLOQUET CELL DIMENSION
C B = STRIP SIZE
      WRITE(*,*) ' ** ENTERING MAIN PROG **'
      WRITE(*,*) ' HOW MANY ITERATIONS DO YOU WISH TO
PERFORM?'
      READ (*,*) CYCLES
      WRITE(*,*) ' INPUT FLOQUET CELL SIZE, STRIP SIZE
'
      WRITE(*,*) ' NORMALIZED IN WAVELENGTHS '
      READ(*,*) A,B
      WRITE(*,*) 'INPUT THE POWER OF 2 YOU WOULD LIKE
TO DIVIDE'
      WRITE(*,*) 'A QUADRANT OF THE WAVEFRONT INTO'
      READ(*,*) NPWTWO
      NTHMAX=2**NPWTWO
       WRITE(*,*)'INPUT THE DISTANCE OF THE SOURCE FROM
THE'
     X,' GRID, NORMALIZED IN WAVELENGTHS'
       READ(*,*) RADIUS
C FREQ = FREQUENCY IN HZ
      WRITE(*,*) ' INPUT FREQUENCY IN HZ'
      READ(*,*) FREQ
C MAX = FFT SIZE = NUMBER OF SAMPLES PER CELL
C IW = LOG2(MAX) ; i.e. MAX = 2**IW
      MAX=32
```

```
      IW=5
C THE STRIPS WILL HAVE INFINITE CONDUCTANCE OR ZERO
IMPEDANCE
      Z=(0,0)
C TH = THETA ANGLE OF INCIDENCE
C PH = PHI ANGLE OF INCIDENCE
C INITIALIZE ROUTINE CONSTANTS
      PI=3.141593
      TPI=2*PI
      C=2.997956E8
      UU=4.0E-7*PI
      EP=8.854E-12
      ETA=SQRT(UU/EP)
      J=(0.0,1.0)
      ALAMB=C/FREQ
      RD=180.0/PI
      DR=1.0/RD
      K=TPI/ALAMB
      K2=K*K
      W=TPI*FREQ
C
C
       WRITE(*,*)'INPUT PHI, 0 or 90'
       READ(*,*) PH
      WRITE(*,*)'TO PRINT OUT THE DATA FOR EACH PLANAR
SEGMENT'
     X,'ENTER A "1", TO SKIP ENTER "0"'
      READ(*,*) IANSWR
C
       WRITE(*,*)
       WRITE(*,*)'SECANT ALGORITHIM APPLIED'
C
C
C
C CALCULATE THE NUMBER OF SAMPLES ON THE STRIP AND IN
THE APERATURE
      TAU=A-B
      N=IFIX(TAU/A*FLOAT(MAX))
      N1=N+1
      WRITE(*,*)
      WRITE (*,10)A,B,TAU
      WRITE(*,15)FREQ,PH,N,MAX
      WRITE(*,*)
10    FORMAT('-','A=',E10.5,'  B=',E10.5,'  TAU=',
E10.5)
15    FORMAT('-','FREQ=',E10.3,' PHI=',E10.4,' N=',I5,'
MAX=',I5)
      IF(N1.GT.MAX) GOTO 900
C
      IF (IANSWR.EQ.1) THEN
```

```
      WRITE(*,*)'        ITHETA      ITER      THETA
REF'
     X,'         CREF'
      WRITE(*,*)
      END IF
C
C THIS SECTION CALCULATES THE REFL. COEF. FOR NTHMAX
INFINITE
C PLANER SEGMENTS
C
C ITHETA IS THE ith CELL STARTING WITH ZERO DEGREES
C SPANNING AN ANGLE TH WRT THE NORMAL
      DO 500 ITH=1,NTHMAX
      CONVERGED=.FALSE.
      ITER=0
      REFM1=0
      ITHETA=ITH-1
      TH=90*FLOAT(ITHETA)/NTHMAX
C
      ALPHA=TPI*(RADIUS-RADIUS*COS(TH*DR))
C
C CALCULATE THE INCIDENT ELECTRIC AND MAGNETIC FIELD
COMPONENTS
C FOR THE ELECTRIC FIELD PARALLEL TO THE WIRES, i.e. NO
CROSS-
C POLARIZATION INCLUDED
      IF (PH.LT.45) THEN
      EINC=COS(ALPHA)+J*SIN(ALPHA)
      STH=0
      HI=EINC/ETA*COS(TH*DR)
      ELSE
      EINC=COS(TH*DR)*(COS(ALPHA)+J*SIN(ALPHA))
      STH=TH

HI=(COS(ALPHA)+J*SIN(ALPHA))/ETA*(COS(TH*DR)+J*SIN(TH*D
R))
      END IF
C
C
      SK=K*SIN(TH*DR)*COS(PH*DR)
      SSK=K*SIN(TH*DR)*SIN(PH*DR)
C CALCULATE GREEN FUNCTION TRANSFORM
      DO 70 I=1,MAX
      IF (I.GT.MAX/2+1) GOTO 30
      U=TPI*(I-1)/A-SK
      GOTO 40
30    U=TPI*(I-MAX-1)/A-SK
40    U=U*U+SSK*SSK
      IF(U.GE.K2) GOTO 50
      G(I)=-J*SQRT(K2-U)
      GOTO 60
```

```
50    G(I)=-SQRT(U-K2)
60    G(I)=G(I)-SSK*SSK/G(I)
70    CONTINUE
C INITIAL E FIELD ESIMATE
      DO 80 I=1,MAX
80    E(I)=(1.0,0.0)
      CALL TRCOPR(E,N1)
      DO 90 I=1,MAX
90    GUESS(I)=E(I)+(0.1,0.0)
C NOTE....ITERATIVE FORM USED IN THIS PROGRAM IS X=AX+B
C CALCULATE B PORTION OF ITERATIVE EQUATION
      DO 100 I=1,MAX
100   CK1(I)=HI*J*W*UU
      CALL FFT(CK1,IW)
      DO 110 I=N1,MAX
110   CK2(I)=HI*W*UU/J
      DO 130 I=1,N
130   CK2(I)=(0.0,0.0)
      CALL FFT(CK2,IW)
      DO 140 I=1,MAX
140   CK(I)=(CK1(I)+CK2(I))/G(I)
C
C     THE FOLLOWING SECTION IMPLIMENTS THE SECANT
METHOD
C
C THE BELOW CONTINUE IS THE START OF A LOOP USING ITER
150   CONTINUE
      ITER=ITER+1
      DO 160 I=1,MAX
      FI(I)=E(I)
      FIM1(I)=GUESS(I)
      EHOLD(I)=E(I)
160   CONTINUE
      CALL FNCTZ(FI,MAX,CONVERGED)
      CALL FNCTZ(FIM1,MAX,CONVERGED)
      DO 170 I=1,MAX
      E(I)=E(I)-FI(I)*((E(I)-GUESS(I))/(FI(I)-FIM1(I)))
170   CONTINUE
      DO 180 I=1,MAX
      GUESS(I)=EHOLD(I)
180   CONTINUE
      IF(ITER.GT.CYCLES.OR.CONVERGED) GOTO 190
      GOTO 150
C THE ABOVE GOTO RETURNS LOOP TO INCREMENT ITER
C
C     THE SECANT METHOD ENDS HERE
C
190   CONTINUE
C
       IF (IANSWR.EQ.1) THEN
      WRITE(*,*)ITHETA,ITER,TH,REF(ITH),CREF(ITH)
```

```
      END IF
C
500   CONTINUE
C
C THIS SECTION CALCULATES THE REFLECTION COEFFICIENT
FOR DIVIDING
C THE WAVEFRONT INTO 2 TO 2 X NTHMAX PLANER SEGMENTS,
TO COMPARE
C THE CONVERGENCE OF THE REF COEF AS THE WAVEFRONT IS
DIVIDED
C INTO MORE AND MORE PLANER SEGMENTS
C
       WRITE(*,*)
C
       DO 570 ITWO=1,NPWTWO
       SUMREF=0
      COMPREF=(0.0,0.0)
       JPWR=2**ITWO
       JSTEP=NTHMAX/JPWR
       DO 550 KSTEP=1,NTHMAX,JSTEP
       SQRREF=REF(KSTEP)*REF(KSTEP)
      CRF=CREF(KSTEP)
       IF (KSTEP.EQ.1) GOTO 540
       SQRREF=2*SQRREF
      CRF=2*CRF
540    SUMREF=SUMREF+SQRREF
      COMPREF=COMPREF+CRF
550   CONTINUE
      ITSEGM=2*JPWR-1
      RESREF=SQRT(SUMREF/ITSEGM)
      OAREF=CABS(COMPREF/ITSEGM)
      IF (ITWO.EQ.1) THEN
      WRITE(*,*)'# OF SEGMENTS  REFLECTION     ABSOLUTE
VALUE   '
     X,'          COMPLEX'
      WRITE(*,*)'IN WAVEFRONT   COEFFICIENT    OF
COMPLEX       '
     X,'          REFLECTION'
      WRITE(*,*)'               COMBINED FROM
REFLECTION      '
     X,'          COEFFICIENT'
      WRITE(*,*)'               AMPLITUDES
COEFFICIENT     '

WRITE(*,*)'_____________________________________________
  '
—    X,'_____________________________'
      END IF
      WRITE(*,*)ITSEGM,'   ',RESREF,OAREF,COMPREF/ITSEGM
570   CONTINUE
```

```
C
      WRITE(*,*)
C
C
C
C
      WRITE(*,*)
      WRITE(*,600)
600   FORMAT('-',10X,'T I M E L Y    E X I T')
      GOTO 9999
900   WRITE(*,910)
910   FORMAT('-',' E R R O R   I N    N')
9999  STOP
      END
C
C
C
C     THIS SUBROUTINE PRODUCES THE VECTOR WE WANT TO
ZERO
C
C
C
      SUBROUTINE FNCTZ(E,MAX,CONVERGED)
      COMPLEX E(32),HOLD(32)
      LOGICAL CONVERGED
      DO 200 I=1,MAX
      HOLD(I)=-E(I)
200   CONTINUE
      CALL XFORM(E,CONVERGED)
      DO 210 I=1,MAX
      E(I)=E(I)+HOLD(I)
210   CONTINUE
      RETURN
      END
C
C
C
C     THIS SUBROUTINE IMPLIMENTS THE TRANSFORMATION ON
THE E FIELD
C
C
C
      SUBROUTINE XFORM(E,CONVERGED)
      COMPLEX E(32),G(32),JC(32),CK(32)
      COMPLEX RI,CREF,HI,J,Z,EINC
      REAL REF,REFM1,REFM2
      LOGICAL CONVERGED
      COMMON RI,CREF(1025),HI,EINC
      COMMON JC,G,J,Z,CK
      COMMON
N,N1,IW,MAX,W,UU,STH,DR,REF(1025),ITH,ITHETA,ITER
```

```
C     CALCULATE FIELD ON STRIP DUE TO FINITE
CONDUCTIVITY
      DO 220 I=N1,MAX
220   E(I)=-JC(I)*Z*B
C     START BY PERFORMING THE INITIAL TRANSFORMATION
      CALL FFT(E,IW)
      DO 230 I=1,MAX
230   E(I)=CONJG(E(I)*G(I))
C PERFORM INVERSE TRANSFORM OF (G*E)
      CALL FFT(E,IW)
C PERFORM THE TRUNCATION OPERATION T(G*E)
      CALL TRCOPRC(E,N)
      DO 240 I=N1,MAX
      E(I)=CONJG(E(I))/MAX
C CALCULATE THE CURRENT DENSITY ON THE STRIP
240   JC(I)=E(I)*J/W/UU-HI
C PERFORM INVERSE TRANSFORMATION ON T(G*E)
      CALL FFT(E,IW)
C PERFORM T(G*E)/G AND ADD CONSTANT "B"
      DO 250 I=1,MAX
      E(I)=E(I)/G(I)+CK(I)
250   CONTINUE
C
C
C
C CALCULATE REFLECTION COEFFICIENT
      TOL=0.0001
      REFM2=REFM1
      REFM1=REF(ITH)
      RI=J*SIN(STH*DR)/COS(STH*DR)
      CREF(ITH)=(E(1)/MAX+EINC)+J*SIN(STH*DR)*
     XABS(1.0-ABS(E(1)/MAX+EINC))
      CREF(ITH)=CREF(ITH)/(COS(STH*DR)+J*SIN(STH*DR))
      REF(ITH)=CABS(CREF(ITH))
      CHECK1=ABS(REF(ITH)-REFM1)
      CHECK2=ABS(REF(ITH)-REFM2)
      IF (CHECK1.LT.TOL.AND.CHECK2.LT.TOL) THEN
255   CONVERGED=.TRUE.
      END IF
C
C
      DO 260 I=1,MAX
      E(I)=CONJG(E(I))/MAX
260   CONTINUE
C PERFORM INVERSE TRANSFORMATION TO OBTAIN FIRST
ITERATED
C ELECTRIC FIELD
      CALL FFT(E,IW)
      DO 270 I=1,MAX
270   E(I)=CONJG(E(I))
      RETURN
```

```
      END
C
C
C
      SUBROUTINE TRCOPR(E,N)
      COMPLEX E(32)
      DO 300 I=N,32
      E(I)=(0.0,0.0)
300   CONTINUE
      RETURN
      END
C
C
C
      SUBROUTINE TRCOPRC(E,N)
      COMPLEX E(32)
      DO 350 I=1,N
      E(I)=(0.0,0.0)
350   CONTINUE
      RETURN
      END
C
C
C
      SUBROUTINE FFT(A,M)
C THIS IS THE FFT SUBROUTINE CALLED FOR FROM THE MAIN
PROGRAM
      COMPLEX A(32),U,W,T
      N=2**M
      NV2=N/2
      NM1=N-1
      J=1
      DO 420 I=1,NM1
      IF(I.GE.J) GOTO 400
      T=A(J)
      A(J)=A(I)
      A(I)=T
400   K=NV2
410   IF(K.GE.J) GOTO 420
      J=J-K
      K=K/2
      GOTO 410
420   J=J+K
      PI=3.141592653589793
      DO 440 L=1,M
      LE=2**L
      LE1=LE/2
      U=(1.0,0.0)
      W=CMPLX(COS(PI/LE1),SIN(PI/LE1))
      DO 440 J=1,LE1
      DO 430 I=J,N,LE
```

```
      IP=I+LE1
      T=A(IP)*U
      A(IP)=A(I)-T
430   A(I)=A(I)+T
440   U=U*W
      RETURN
      END
C
C
C
      COMPLEX FUNCTION SINHH(X)
      COMPLEX X
      SINHH=0.5*(CEXP(X)-CEXP(-X))
      END
C
C
C
      COMPLEX FUNCTION COSHH(X)
      COMPLEX X
      COSHH=0.5*(CEXP(X)+CEXP(-X))
      END
```

REFERENCES

[1] Wait, J.R."Theory of Scattering from Wire Grids and Mesh Structures." In Electromagnetic Scattering pp. 253-288. Edited by P. Uslenghi. New York: Academic Press, 1978.

[2] Larsen, T. "A Survey of the Theory of Wire Grids." I.R.E. Transactions on Microwave Theory and Techniques (May 1962): 191-201.

[3] Tsao, C. and Mittra, R. " A Spectral-iteration Approach for Analyzing Scattering from Frequency Selective Surfaces." IEEE Transactions on Antennas and Propagation. AP-30 (January 1982): 303-308.

[4] Brand, J.C. "On the Converegnce of an Iterative Formulation of Electromagnetic Scattering From an Infinite Grating of Thin Wires." Ph.D Disertation, Dept. of Electrical and Computer Engineering, North Carolina State University, Rayleigh, North Carolina, May 1985.

[5] Christodoulou, C.G. and Kaufman, J.F."On the Electromagnetic Scattering from Infinite Rectangular Grids with Finite Conductivity." IEEE Transactions on Antennas and Propagation. AP-34 (February 1986): 144-154.

[6] Sarkar, T.P. and Rao, S.M. "The Application of the Conjugate Gradient Method for the Solution of Electromagnetic Scattering from Arbitrary Oriented Wire Antennas."IEEE Transactions on Antennas and Propagation. AP-32 (April 1984): 398-402.

[7] Montgomery, J.P. and Davey, K.R. "Conjugate Gradient Solution of Arbitrary Planar Frequency Selected Surfaces." Int'l URSI-Symposium Boston: p. 155, 1984.

[8] Otteni, G.A. " Plane Wave Reflection from a Rectangular-Mesh Ground Screen" IEEE Transaction on Antennas and Propagation. AP-2 (November 1973): 843-851.

[9] Hill, D.A. and Wait, J.R. "Electromagnetic Scattering of an Arbitrary Plane Wave by Two Nonintersecting Perpendicular Grids", Canadian Journal of Physics 52 (1974): 227-237.

[10] Amitay, N. and Galindo, V."The Analysis of Circular Waveguide Phased Arrays."Bell Systems Technical Journal, 47 (November 1968): 1903-1933.

[11] Froberg, C.E. Introduction to Numerical Analysis Reading, Massachusetts: Addison-Wesley Publishing Company, 1965.

[12] Jackson, J.D., Classical Electrodynamics New York: John Wiley & Sons, 1975.

[13] Hecht, E. and Zajac, A. Optics Readings, Massachusetts: Addison-Wesley Publishing Company, Inc., 1974.

[14] Cwik, T. and Mittra, R. " Scattering from a Finite Strip Grating: The Effect of Curvature." AP-S 1986 International Symposium Digest p. 281, Philadelphia, June 1986.

[15] Wait, J.R. "Reflection at Arbitrary Incidence from a Parallel Wire Grid." Applied Scientific Research 4B (1954): 339-400.